Functional differentiation of invasive and native plants along a leaf efficiency/safety trade-off

Francesco Petruzzellis[1,2]*, Enrico Tordoni[1,3], Martina Tomasella[1], Tadeja Savi[4], Vanessa Tonet[5], Chiara Palandrani[2], Miris Castello[1], Andrea Nardini[1] and Giovanni Bacaro[1]

[1]University of Trieste, Department of Life Sciences, via L. Giorgieri 10, 34127, Trieste, Italia

[2]University of Udine, Department of Agricultural, Food, Environmental and Animal Sciences, via delle Scienze 206, 33100, Udine, Italy

[3]University of Tartu, Institute of Ecology and Earth Sciences, Department of Botany, Lai 40, Tartu 51005, Estonia

[4]Department of Integrative Biology and Biodiversity Research, University of Natural Resources and Life Sciences, Vienna (BOKU), Institute of Botany, Gregor-Mendel-Straße 33, 1190 Vienna, Austria

[5]University of Tasmania, School of Biological Sciences, Private Bag 55, Hobart, TAS, 7001, Australia

*corresponding author: francesco.petruzzellis@uniud.it; ORCID: https://orcid.org/0000-0002-3635-8501

FUNDING

This work is part of the project 'Functional traits as a tool to predict invasive potential by alien species in different native communities', funded by University of Trieste (Finanziamenti per la Ricerca di Ateneo 2015).

AUTHOR CONTRIBUTIONS

FP, AN and GB designed and planned the experiment and the sampling campaigns; FP, ET and MC identified sampling sites and species; FP, ET, MT, TS, VT and CP collected the data; FP, ET and GB performed the statistical analysis; FP led the writing of the manuscript with inputs from AN and GB, all authors revised and agree with the final version of the manuscript.

HIGHLIGHTS

- Invasive species have lower leaf construction costs and drought resistance
- Invasive species have a denser leaf venation network on a mass basis
- Invasive species share similar traits irrespective of growth form and site type
- Hydraulic and venation traits underlie invasive potential of invasive species

ABSTRACT

Plant invasive alien species (IAS) are a serious threat to biodiversity. Several studies have compared the functional features of IAS and native species to identify the functional traits, or set of traits, favouring the process of invasion. However, most of these studies analysed traits only related to carbon and nutrients, and the inclusion of traits related to water use and acquisition might be useful to describe the functions underlying plant invasion. Here we present an analysis of cost-related, hydraulic and leaf vein traits measured on a large assemblage of woody and herbaceous native and invasive species (93 species in total, 78 natives and 15 IAS), that co-occur in site types in the Mediterranean area with different water availability (i.e. xeric, mesic and hydric sites). IAS shared lower leaf construction costs and drought resistance, but potential higher efficiency in water transport (i.e. higher values of vein length per unit area/mass) than native species. Moreover, IAS and native species separated along the trade-offs drawn by the measured traits, suggesting that hydraulic and vein traits could set an important axis of variation between IAS and native species. At last, IAS tended to occupy the fast-growth region of the functional space, independently of growth form and site type. Hydraulic and vein traits provide stronger mechanistic linkages between construction costs and photosynthetic and growth rates, thus possibly playing a central role in determining the invasive potential of IAS. IAS could reduce costs associated with leaf construction and resistance to drought stress having, at the same time, high efficiency of water transport and photosynthetic rates by developing a denser venation network, translating to higher growth rates than native and more conservative species.

KEYWORDS:

Drought resistance; Hydraulic Safety-Efficiency trade-off; Invasive Alien Species; Leaf economic spectrum; Mechanistic traits; Turgor loss point; Leaf venation

1. INTRODUCTION

The accidental or deliberate introduction of exotic plant species in natural habitats is a potential threat to biodiversity conservation (Hulme, 2011). Most introduced plant species fail to establish persistent population and thus frequently go largely unnoticed. However, some of them can profit from favourable ecological conditions and lack of effective competitors, predators, or pathogens to spread rapidly over large areas in the new range, thus becoming invasive (*sensu* Richardson et al., 2000). Invasive alien species (IAS) are among the major causes of biodiversity loss at a global scale, justifying the ever-increasing efforts devoted to identifying the functional traits, or set of traits, favouring the process of invasion (Reich, 2014; Wright et al., 2004).

Among the several important physiological traits setting the limits of plant productivity and competitive ability in different habitats, those included in the "Leaf Economic Spectrum" or LES (Wright et al., 2004) are particularly useful. Indeed, LES traits capture the most relevant trade-offs between species-specific relative growth rates, stress tolerance, mechanical reinforcement, and longevity of leaves (Onoda et al., 2017; Reich, 2014; Wright et al., 2004). Specifically, fast-growing (or acquisitive) species tend to have lower leaf mass per unit area (LMA), higher light-saturated rates of photosynthesis per unit mass (A_{mass}) and higher nitrogen concentration per unit mass (N_{mass}), but shorter leaf lifespan (LL) relative to slow-growing (or conservative) species (Leishman et al., 2007; Penuelas et al., 2009; van Kleunen et al., 2010). Other important trade-offs have been described in terms of species-specific water use strategies and drought tolerance, which are among the most important drivers of species distribution and abundance within and across biomes (Bartlett et al., 2016; Bartlett et al., 2012a; Larter et al., 2017). Traits associated with plant water relations such as the water potential inducing 50% loss of organ hydraulic conductivity (Ψ_{50}), or the water potential inducing cell turgor loss (Ψ_{tlp}) are particularly useful as reliable metrics of species-specific drought tolerance (Bartlett et al., 2012a). Species occupying water-limited habitats typically display low values of Ψ_{50} and Ψ_{tlp} coupled to intrinsically low growth rates (Bartlett et al., 2012a; Lenz et al., 2006; Zhu et al., 2018). This arises from the fact that one of the determinants of plant growth rate and productivity is the efficiency of root-to-leaf water transport, generally expressed in terms of plant and organ hydraulic conductivity (Brodribb, 2009). In particular, stem and leaf hydraulic conductivity (K_{stem} and K_{leaf}, respectively) are strongly positively correlated to plant's productivity (Fan et al., 2012; Zhang & Cao, 2009). All the above hydraulic and water relations traits are apparently coordinated in the "hydraulic safety-efficiency" trade-off (HSE) (Gleason et al., 2016; Nardini & Luglio, 2014, Ocheltree et al., 2016), whereby species with higher resistance to drought (i.e. lower values of Ψ_{50} and Ψ_{tlp}) tend to display lower hydraulic efficiency (i.e. lower K_{stem} and K_{leaf}). Although significant, this trade-off was

weak when considering a global database of woody species but resulted stronger within families spanning a large range in habitat aridity (Gleason et al., 2016) or in a smaller dataset of herbaceous C4 species (Ocheltree et al., 2016). This suggested that the HSE trade-off may not have contributed to the divergence of species on a global scale (Gleason et al., 2016), but it may have a stronger effect when closely spatially related species are considered.

Recent studies have revealed several interesting trade-offs between LES and hydraulic traits. As an example, species with lower Ψ_{tlp} are also characterized by higher LMA and longer leaf lifespan (LL), suggesting that leaf turgor maintenance in water-limited habitats comes at the cost of significant carbon investment for leaf construction (Villagra et al., 2013) or accumulation of non-structural carbohydrates (Poorter et al., 2009). In turn, gas exchange rates, photosynthetic capacity and growth rates are correlated with the efficiency of water transport across the plant body. In fact, species with higher K_{leaf} also display higher photosynthetic and growth rates (Sack et al., 2013; Scoffoni et al., 2016). Despite that, hydraulic traits such as Ψ_{50} and K_{leaf} have only been seldom included in studies accounting for a high number of species or replicates, because of the time-consuming nature of their measurement. However, recent developed frameworks have allowed faster and reliable measurements of Ψ_{tlp} (Bartlett et al., 2021b; Griffin-Nolan et al., 2019; Petruzzellis et al., 2019), which is coordinated with Ψ_{50} both at leaf and stem level (Zhu et al., 2018). Moreover, Sack et al. (2013) have proposed a "flux trait network" model to describe the mechanistic coordination between leaf vein architecture, K_{leaf} and LES traits. In this framework, species with higher vein length per unit leaf area (VLA) or per leaf mass (VLM) have also higher K_{leaf} and, in turn, higher photosynthetic and growth rates. Considering the coordination between Ψ_{50} and Ψ_{tlp} and the relationships described in the "flux trait network", Ψ_{tlp} and vein traits could be considered as mechanistically coordinated with hydraulic safety and efficiency respectively, and we propose to consider them as HSE-related traits.

The trade-offs among LES, HSE and leaf vein traits might be at the basis of the "fast-slow plant economic spectrum" proposed by Reich (2014), and their integration could be useful to highlight fundamental functions underlying plants growth strategies. Several comparative analyses of functional traits between native and IAS have emphasized that the latter tend to share values of LES traits that favour fast growth (Leishman et al., 2014; Pyšek & Richardson, 2008). IAS typically have high values of traits related to growth performance (i.e. photosynthetic rate, size) and low values of traits associated with carbon-costs for construction of plant organs (i.e. LMA, wood density) (van Kleunen et al., 2010). Thus, trait divergence has been suggested to enhance the invasion success of alien species (Divíšek et al., 2018; Marchini et al., 2019; Tordoni et al., 2020), but the direction of traits differences was not always consistent. In fact, the invasion process is considered strongly context dependent (Funk et al., 2016), and multiple suites of traits might promote IAS spread in different environments. IAS

with more acquisitive traits than native species seemed to be advantaged in high-resource habitats, while IAS with more conservative traits are reported as successful in environments with low resource availability (Funk, 2013; Funk & Vitousek, 2007). More recently, Divíšek et al. (2018) suggested that IAS tend to occupy the edge of the trait space in different habitats, defined as the periphery of the plant functional traits space represented in each habitat. As suggested by Hulme & Bernard (2018), studies at regional scales along suitable environmental gradients, considering the full plant community and including traits chosen based on *a priori* knowledge of their function and response to environmental and/or biotic drivers, are needed to better understand how and if IAS and native species differ. In this light, HSE and HSE-related traits might be hypothesized to set an important axis of variation between invasive and native species, especially in water-limited environments, and their measurement could help to unravel the central functions underpinning plant invasion mechanisms. Previous studies reported that native and invasive species have different water use, with native species generally adopting a more conservative strategy (Antunes et al., 2018; Cavaleri et al., 2014; Cavaleri & Sack, 2010). Morevoer, some studies have shown that IAS could maintain higher photosynthetic rates than native species during drought periods, absorbing relatively large amounts of water and drying the adjacent soil through transpiration (Cavaleri & Sack, 2010; Vasquez-Valderrama et al., 2020). This ability may arise from higher efficiency of water transport (higher K) or thanks to higher root density and depth in IAS, indicating the need for further detailed comparative analyses of hydraulic traits between native and IAS (Pintó-Marijuan & Munné-Bosch, 2013).

To date, few studies dealing with plant invasion have analysed HSE or HSE-related traits, with contrasting results. Crous et al. (2012) found that in riparian zones of South Africa, the invasive *Acacia mearnsii* had higher resistance to xylem embolism formation (lower Ψ_{50}) than co-occurring native species, and similar results were reported for saplings of *Psidium cattleianum* (Yazaki et al., 2010), grown from seeds collected in Bonin Island (Japan). Zeballos et al. (2014) compared water transport strategies of 8 IAS and 12 native species of xerophytic woodlands in Central Argentina and reported that IAS had hydraulic traits associated with higher water transport efficiency than native species. In a recent study, Díaz de León Guerrero et al. (2020) found that in urban Mediterranean ecosystem IAS had lower vessel density and wider vessel diameters than native species, which are traits associated with higher hydraulic conductance but higher risk of xylem embolism formation (Hacke et al., 2017). Similarly, in Classical Karst (NE Italy), the invasive tree *Ailanthus altissima* had higher hydraulic conductivity and vulnerability to embolism than the co-occurring native *Fraxinus ornus* (Petruzzellis et al., 2018). Regarding herbaceous communities, Tordoni et al. (2019) found that plot-level community weighted mean (CWM) values of Ψ_{tlp} and minor vein length per unit area (VLA_{min}) for a sampled pool of IAS in a coastal ecosystem are higher than those calculated on

native species. Despite some discrepancies, all these studies suggest that HSE traits might consistently differ between IAS and native species, and their inclusion in comparative studies along with LES and vein traits might provide novel insights into the functional mechanisms of plant invasions.

Here we present an analysis of LES, HSE and leaf vein traits measured on a large assemblage of woody and herbaceous native and invasive species (93 species in total, 78 natives and 15 IAS), that co-occur in habitats in the Mediterranean area with different water availability. Specifically, we tested the following hypotheses: *i*) IAS share lower leaf construction costs and drought resistance, but higher efficiency in water transport (i.e. higher values of vein traits) than native species; *ii*) LES and HSE-related are coordinated in trade-offs, and *iii*) IAS and native species occupy different spaces along the trade-offs drawn by these traits. We hypothesized that species with low construction costs also have lower drought resistance and higher vein length per unit mass/area and that, while native species spread along traits trade-offs, IAS tend to cluster in the acquisitive portion of the functional space.

2. METHODS

2.1 Study sites and sampling design

Sampling site types were selected in North-East Italy, along a gradient of water availability (xeric, mesic and hydric site types, see Fig. S1 and S2 in Appendix A) over a region of ~1500 km^2 encompassing different environments such as coastal dunes, wetlands, arid grasslands and woodlands. The climate of the study area is transitional between the Mediterranean and continental type (Poldini et al., 1992), thus favouring the co-existence of ecologically very diverse plant communities. Three pairs of sampling sites (each pair composed by one woody and one herbaceous site) were selected, for a total of six sites. A summary of climatic data is reported in Tab. S1 in Appendix A.

Two sites, one for woody species and one for herbaceous ones (extending for ~0.8 and ~1.5 km^2, respectively), were characterized by pronounced xericity, as they were located in coastal areas dominated by typical Mediterranean woody evergreen species (Illyrian holm oak woodland*)* or by sand dunes hosting vegetation typical of European coastlines (e.g. *Cakile maritima*, *Agropyron junceum*, *Ammophila arenaria*).

Mesic sites were located in the Classical Karst, a limestone plateau belonging to the NW Dinaric area located immediately north of the Adriatic Sea, and the nearby coastal/lowland areas. These sites were characterized by very high permeability (Urbanc et al., 2012) and by shallow soil (< 30 cm) overlying a carbonate bedrock dominated by limestone and dolostone (Nardini et al., 2021). Here, we identified two sampling sites, one (extending for ~1 km^2)

dominated by mesic vegetation comprising mixed deciduous thermophilous oak woodland dominated by *Quercus pubescens*, *Fraxinus ornus, Ostrya carpinifolia* and *Prunus mahaleb* (Poldini, 1989). The other site (extending for ~0.5 km^2) was characterised by typical herbaceous communities represented by karstic grasslands, where the dominant species are *Bromopsis erecta* and *Chrysopogon gryllus*.

Two other sites (extending for ~0.5 and ~0.6 km^2), characterized by a higher water availability, were located in wetlands bordering small lakes and rivers, hosting riparian helophytic vegetation dominated by large sedges (*Carex elata* and *Carex vesicaria*), *Phragmites australis*, *Agrostis stolonifera* and riparian trees, such as *Populus nigra* and *Salix* spp. Specifically, one site (where woody species were sampled) was located in proximity of a river, while the other site was placed on the border of a lake which is flooded during the autumn and winter seasons and it is strongly reduced in spring and summer.

For woody plants, 5 individuals of each native and invasive species present in each site were randomly sampled following Petruzzellis et al. (2017), for a total of 65 individuals. In total, 9 native woody species (dominant species in the region according to Poldini, 1989) and 3 IAS were sampled (see Tab. S2).

For herbaceous species, 22 to 30 squared plots of 16 m^2 were randomly selected in each sampling site, and 2 to 7 individuals for each of the herbaceous species present in each plot was randomly sampled. In total, we sampled 286 individuals of 81 herbaceous species in the 3 herbaceous sites (69 native and 12 invasive species). The complete scheme of the sampling design is summarized in Tab. 1. The native or invasive status was assigned to each species according to the updated checklist of the Italian alien vascular flora (Galasso et al., 2018). Fieldwork activities were carried out in spring-summer months during the years 2016-2018.

Tab. 1. Number of species and individuals (in brackets) of invasive (IAS) and native species sampled in each sampling area.

Sampling area	Invasive species (IAS)		Native species	
	Woody	Herbaceous	Woody	Herbaceous
Xeric	1 (5)	6 (26)	2 (10)	17 (56)
Mesic	1 (5)	1 (5)	5 (25)	29 (103)
Hydric	2 (10)	5 (22)	2 (10)	23 (74)

2.2 Trait measurements

The complete list of LES, HSE-related and leaf vein traits, their associated physiological functions and number of leaves and individuals sampled for each trait are reported in Tab. 2.

Tab. 2. List of functional and mechanistic traits with associated units, trait categories and number of leaves per individuals (in brackets) measured in this study.

Name	Abbreviation	Unit	Trait category	N° leaves (individuals)	
				Woody	*Herbaceous*
Leaf Mass per Area	**LMA**	mg cm^{-2}	LES traits	5 (5)	3 to 9 (2 to 7)
Leaf Dry Matter Content	**LDMC**	mg g^{-1}		5 (5)	3 to 9 (2 to 7)
Leaf N content	$\mathbf{N_{mass}}$	%		1 (5)	3 to 9 (2 to 7)
Leaf osmotic potential at full turgor	$\boldsymbol{\pi_0}$	MPa	HSE-related traits	5 (5)	3 to 9 (2 to 7)
Leaf water potential at turgor loss point*	$\boldsymbol{\Psi_{tlp}}$	MPa		5 (5)	3 to 9 (2 to 7)
Minor vein length per unit area	$\mathbf{VLA_{min}}$	mm mm^{-2}	Vein traits	5 (5)	3 to 9 (2 to 7)
Minor vein length per unit mass	**VLM**	m g^{-1}		5 (5)	3 to 9 (2 to 7)
Leaf ^{13}C isotopic composition	$\boldsymbol{\delta^{13}C}$	‰	Water-use efficiency	1 (5)	3 to 9 (2 to 7)

LES and carbon isotope traits were measured on 5 leaves, randomly sampled from each of the 5 individuals selected (25 leaves in total from each individual) in the 3 sampling sites for woody plants, while for herbaceous species 3 to 9 leaves from each individual were randomly sampled in each site.

Leaf dry matter content (LDMC) and leaf mass per unit area (LMA) were calculated as:

LDMC = Leaf dry weight/Leaf turgid weight (1)

LMA = Leaf dry weight/Leaf area (2)

Fresh leaves were first rehydrated overnight, and leaf turgid weight (without leaf petioles or rachis) was measured with an analytical balance. Then, leaves were scanned, and leaf area

was measured using the software ImageJ (Schneider et al., 2012). Leaves were finally oven-dried for 24 h at 70 °C to obtain their dry weight.

Nitrogen content (N_{mass}) and carbon isotopic composition ($\delta^{13}C$, proxy of water use efficiency) were measured on the same leaves sampled for LMA and LDMC. Leaves were pulverized in a mortar after oven drying. Elemental composition and $\delta^{13}C$ were measured by elemental analyzer/continuous flow isotope ratio mass spectrometry using a CHNOS Elemental Analyzer (vario ISOTOPE cube, Elementar, Hanau, Germany) coupled with an IsoPrime 100 mass spectrometer (Isoprime Ltd, Cheadle, UK). All isotope and elemental composition analyses were performed by the Center for Stable Isotope Biogeochemistry (University of California, Berkeley). Long-term external precision based on reference material "NIST SMR 1577b" (bovine liver) is 0.10‰ and 0.15‰, respectively for C and N isotope analyses.

For HSE-related traits, leaves for the measurement of osmotic potential at full turgor (π_0) and water potential at turgor loss point (Ψ_{tlp}) were collected as described above. Twigs were detached, wrapped in cling film and put in plastic bags containing wet paper inside to avoid dehydration. Samples were stored in cool bags until processing in the laboratory within 2 h from sampling. π_0 and Ψ_{tlp} were determined according to Bartlett et al. (2012b) with some modifications. Twigs bearing leaves were first rehydrated overnight and one leaf per twig was roughly crumbled and sealed in cling film. Then, it was immersed in liquid nitrogen for 2 min. Leaves (still sealed in cling film) were carefully ground and stored in sealed plastic bottles at −20 °C until measurements. Samples were thawed at room temperature for 5 min while still sealed in cling film and in plastic bottles. Measurements of π_0 were done with a dew point hygrometer (π_{0_osm}) (WP4, Decagon Devices Inc.). To overcome possible bias due to dilution or enrichment of solutes of symplastic fluids (Bartlett et al., 2012b), π_0 and Ψ_{tlp} were estimated with the following equations (Petruzzellis et al., 2019):

$$\pi_0 = 0.506\ \pi_{0\_osm} - 0.002LDMC \text{ (expressed in mg g}^{-1}\text{)} \quad (3)$$

Ψ_{tlp} was finally calculated as:

$$\Psi_{tlp} = 1.31\ \pi_0 - 0.03. \quad (4)$$

To quantify leaf vein traits, the length of minor veins (3rd and higher orders) per unit leaf surface area (VLA_{min}) and per unit mass (VLM) were measured as:

$$VLA_{min} = \text{Vein Length/Leaf sample area.} \quad (5)$$

$$VLM = VLA_{min}/LMA \quad (6)$$

Fresh leaves were treated in 1 M NaOH solution for 48-72 h. Then, a portion of 1 cm^2 was cut from the central portion of each leaf (carefully avoiding the midrib) and cleared in 1% NaClO for 5 min. Samples were then dehydrated in a sequence of ethanol solutions at increasing concentrations (25%, 50%, 75% and 100%) and then immersed in an alcoholic solution of toluidine blue (3%) overnight. Samples were rehydrated in a series of ethanol solutions at decreasing concentration and microscopic slides were prepared. Images of leaf portions of ~5 mm^2 were captured with an optical microscope at 4× magnification equipped with a digital camera and VLA_{min} was measured using PhenoVein software (Bühler et al., 2015).

2.3 Statistical Analysis

2.3.1 Single trait differences between native species and IAS

Single-trait differences between native species and IAS were tested using random intercept linear mixed models (LMMs). Specifically, one LMM was run for each functional trait (i.e. response variable) setting the status (2 levels: IAS and native), site type (3 levels: xeric, mesic and hydric) growth form (2 levels: herbaceous and woody) and the interactions status:site type and status:growth form as the fixed effects and species as the random effect. Model's assumptions were visually checked by means of residuals' quantile-quantile Plots (for normality of residuals) and residuals vs fitted values plots (for homoscedasticity assumption). When normality assumption was violated, the response variable was log transformed. LMMs were run using *lmer* function in "lme4" R package (Bates et al., 2015). Model performance was evaluated calculating the conditional and marginal coefficients of determination (pseudo R^2) using the function *r.squaredGLMM*, with Nakagawa and Schielzeth method, available in "MuMIn" R package (Barton, 2020).

2.3.2 Traits' trade-offs calculation

A preliminary screening to highlight possible correlations between traits was performed by calculating pairwise Spearman's *r* correlation coefficient among traits, using *rcorr* function from "Hmisc" package (Harrell, 2019). For $\delta^{13}C$, we calculated the correlations considering only C3 species. P-values for multiple correlations were corrected using "False Discovery Rate" correction through *p.adjust* function in "stats" R package. Only for significant correlations ($p < 0.05$), second-order polynomial LMMs were further calculated, setting the species as the random intercept factor. In the case the quadratic term was not statistically significant, we retained the simple LMM after testing for potential significant change in the residual sum of squares by means of likelihood ratio rest. Additional information about model calculation is provided in Appendix C. For each significant relationship, the occurrence probability of IAS and native species in specific regions of the traits trade-offs was calculated by means of kernel density estimation, using *stat_density2d* function in "ggplot2" package (Wickham, 2016). The

bandwidth parameter was calculated using *bandwidth.nrd* function in MASS R package (Venables & Ripley, 2002), implemented in *stat_density_2d* function, following the procedure described in Venables & Ripley (2002).

2.3.3 Estimation of the functional space and species differentiation patterns

To summarize and visually describe the differences between native and IAS in multivariate functional space, we performed a Principal Component Analysis (PCA) using the R function *princomp*. All values were standardized (zero mean, unit variance) before the analysis, and the number of significant PCA axes to be retained without loss of significance was then calculated (Dray, 2008). To estimate the occurrence probability of IAS and native species in specific regions of the two-dimensional functional space defined by the first two PCA axes, we used two-dimensional density kernel estimation, following the procedure reported in Díaz et al. (2016). Permutational multivariate analysis of variance (PERMANOVA, Anderson, 2001) was run to assess whether factors such as status, growth form and Site type significantly influenced species clustering in the functional spaces drawn by the measured functional traits. Specifically, Euclidean distances between species traits were computed and 3 independent PERMANOVAs were run using *adonis* function in "vegan" R package (Oksanen et al., 2017) using 999 permutations. Status (fixed factor, 2 levels), growth form (fixed factor, 2 levels) and Site type (fixed factor, 3 levels) were selected as explanatory variables. R software version 4.0.2 (R Core Team 2020) was used for all the statistical analyses.

3. RESULTS

The mean values of the different functional traits measured for each species are reported in Table S2. Regarding LES traits, IAS had significantly lower values of LMA (p = 0.001) and higher N_{mass} (p < 0.001), while LDMC did not significantly differ between the two groups (Fig. 1). HSE-related traits, such as π_0 (p = 0.02) and Ψ_{tlp} (p = 0.02) (Fig. 1) and vein traits, represented by VLA_{min} (p = 0.02) and VLM (p = 0.004) were higher in IAS that in native species (Fig. 1). Lastly, water use efficiency estimated in terms of $\delta^{13}C$ did not significantly differ between IAS and native species. A complete summary of model outputs is available in Appendix B.

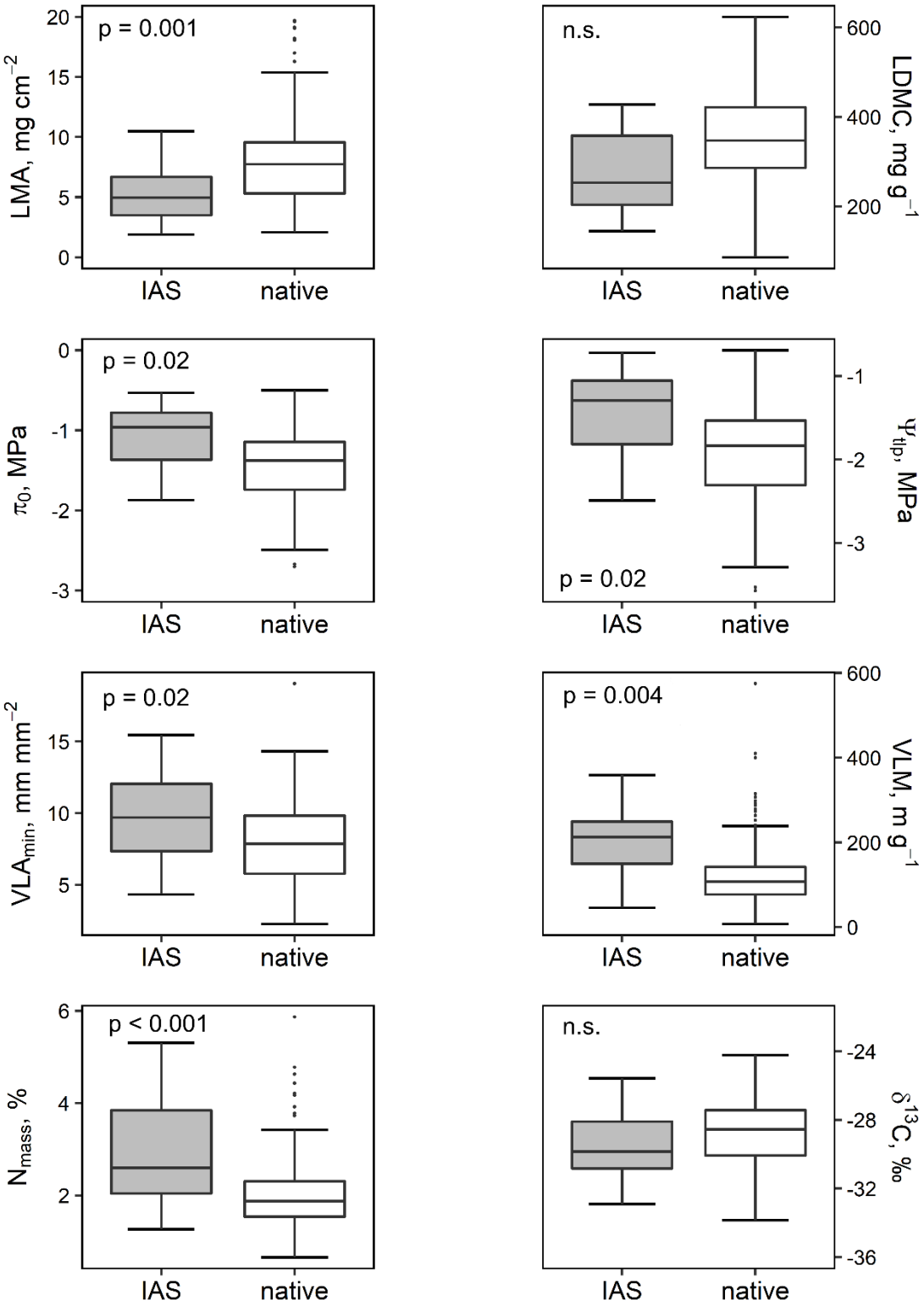

Fig. 1. Boxplots of LMA, LDMC, π_0, Ψ_{tlp}, VLA_{min}, VLM, N_{mass} and leaf C isotopic composition ($^{13}\delta C$) measured in IAS (grey boxes) and native species (white boxes). P-values are reported. n.s. = not significant.

Strong trade-offs were found between LES, HSE-related and water-use efficiency traits (Tab. S3 in Appendix A). LMA was negatively related with Ψ_{tlp}, N_{mass} and VLM and positively with $\delta^{13}C$ (Fig. 2). Moreover, a positive relationship was found between Ψ_{tlp} and N_{mass} and VLM (Fig. 3), while Ψ_{tlp} and $\delta^{13}C$ were negatively related to each other (Fig. 3). Also, VLM was positively related to N_{mass} and negatively with $\delta^{13}C$ (Fig. 4). A complete report of the output of second-order polynomial and simple LMMs of these relationships is reported in Appendix C.

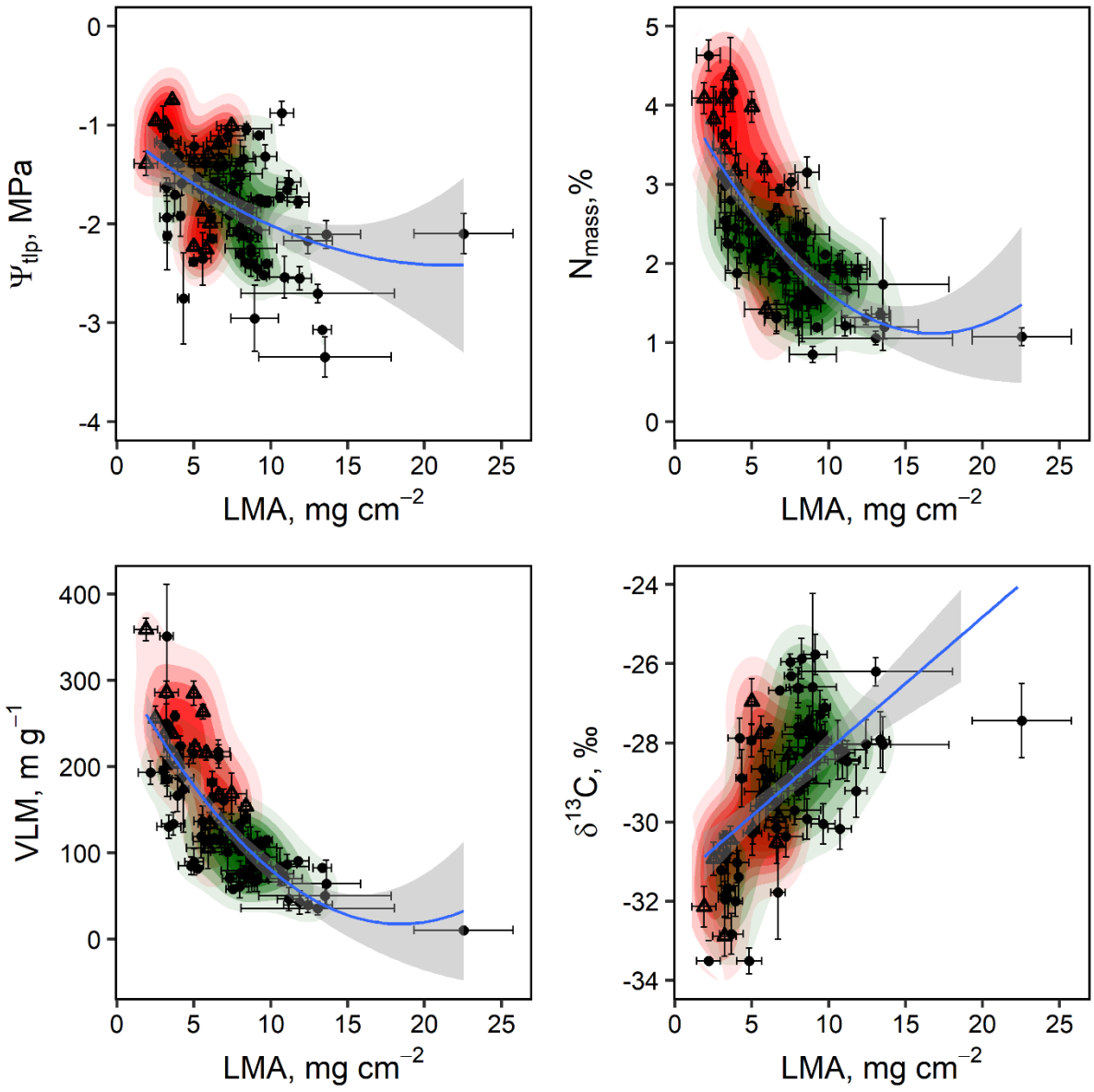

Fig. 2. Relationships between Ψ_{tlp}, N_{mass}, VLM and $\delta^{13}C$ *vs* LMA. Empty triangles indicate IAS, while solid circles represent native species. The colour gradient indicates regions of occurrence probability of native species (green) and IAS (red) along the trade-offs reported. Circles are traits' mean values of each species and error bars represent the associated standard deviation.

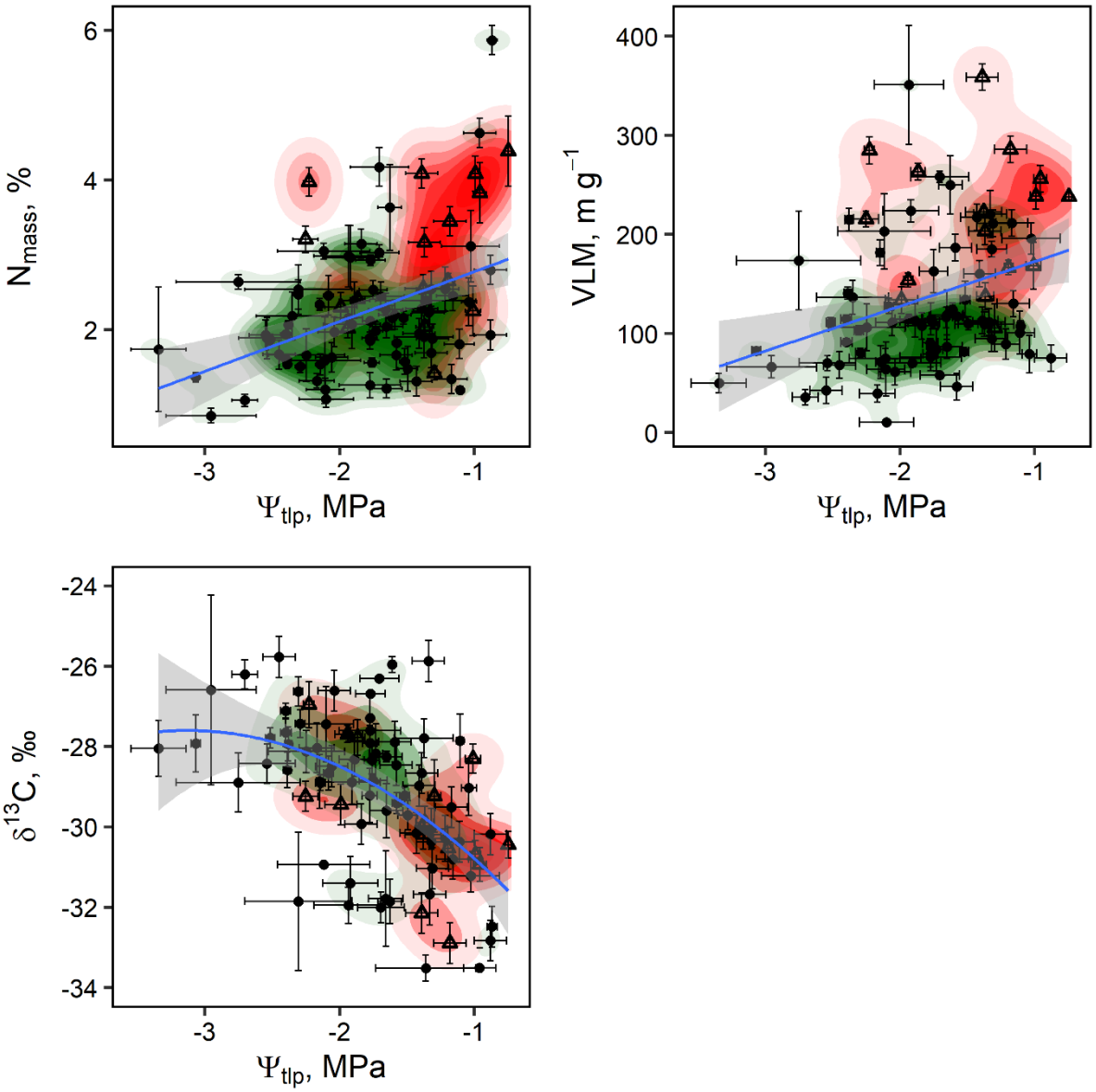

Fig. 3. Relationship between N_{mass}, VLM and $\delta^{13}C$ *vs* Ψ_{tlp}. Empty triangles indicate IAS, while solid circles represent native species. The colour gradient indicates regions of occurrence probability of native species (green) and IAS (red) along the trade-offs reported. Circles are traits' mean values of each species and error bars represent the associated standard deviation.

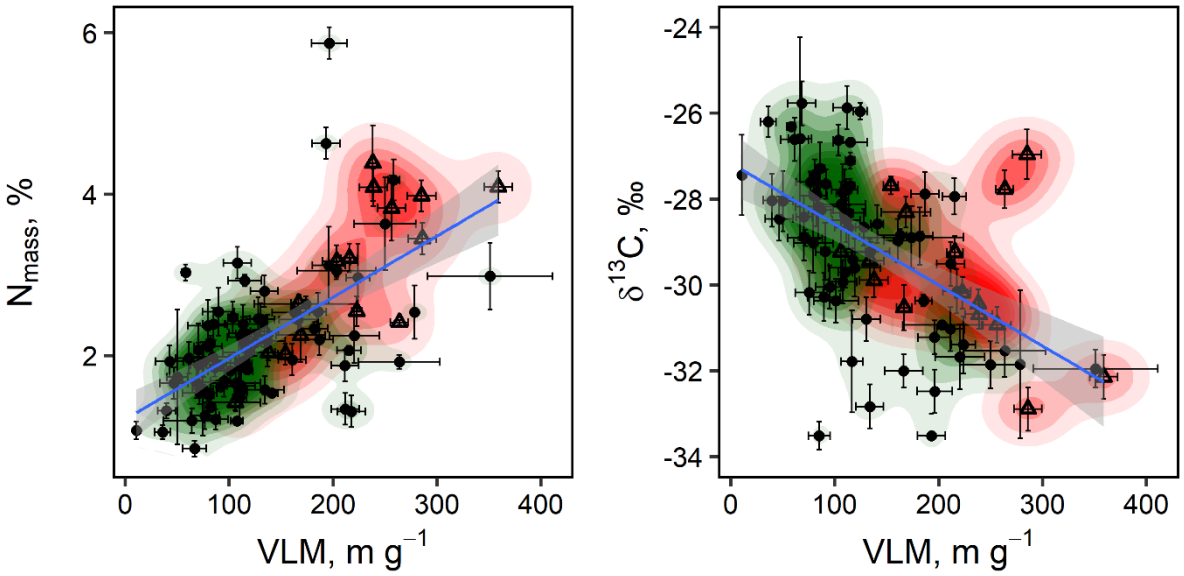

Fig. 4. Relationship between N_{mass} and $\delta^{13}C$ vs VLM. Empty triangles indicate IAS, while solid circles represent native species. The colour gradient indicates regions of highest occurrence probability of native species (green) and IAS (red) along the trade-offs reported. Circles are traits' mean values of each species and error bars represent the associated standard deviation.

Considering the first four PCA axes, the projection of species on PC1 vs PC2 (64.9% of the total variance explained) and on PC1 vs PC4 (54.6% of the total variance explained) revealed a major significant separation between IAS and native species (Fig. 5, see PERMANOVA outputs in Tab. S4 in Appendix A). In general, IAS occupied the region of the functional space associated with acquisitive traits (i.e. higher values of Ψ_{tlp}, N_{mass} VLA_{min} and VLM, and lower values of LMA). The projection of the species on PC1 and PC3 (55.7% of the total variance explained) allowed to separate between C3 and C4 species, along a WUE gradient (Fig. S3 in Appendix A), but not between IAS and native species. At last, PC2 and PC4 (31.9 % of the total variance explained) did not provide any further clear differentiation between IAS and native species (data not shown). When considering different growth forms (Fig. 6a), woody and herbaceous species tended to separate along PC2 (see PERMANOVA outputs in Tab. S4 in Appendix A). Moreover, herbaceous IAS and native species separated along PC1, where IAS clustered in the leftmost part of the multivariate space; in contrast, PC2 showed a net separation of woody IAS and native species (IAS clustered in the upper part of the ordination), as well as of woody and herbaceous IAS (Fig. 6a). Interestingly, when considering different habitats, most IAS shared the functional space associated with natives occurring in hydric sites, regardless of the habitat where they were sampled (Fig. 6b).

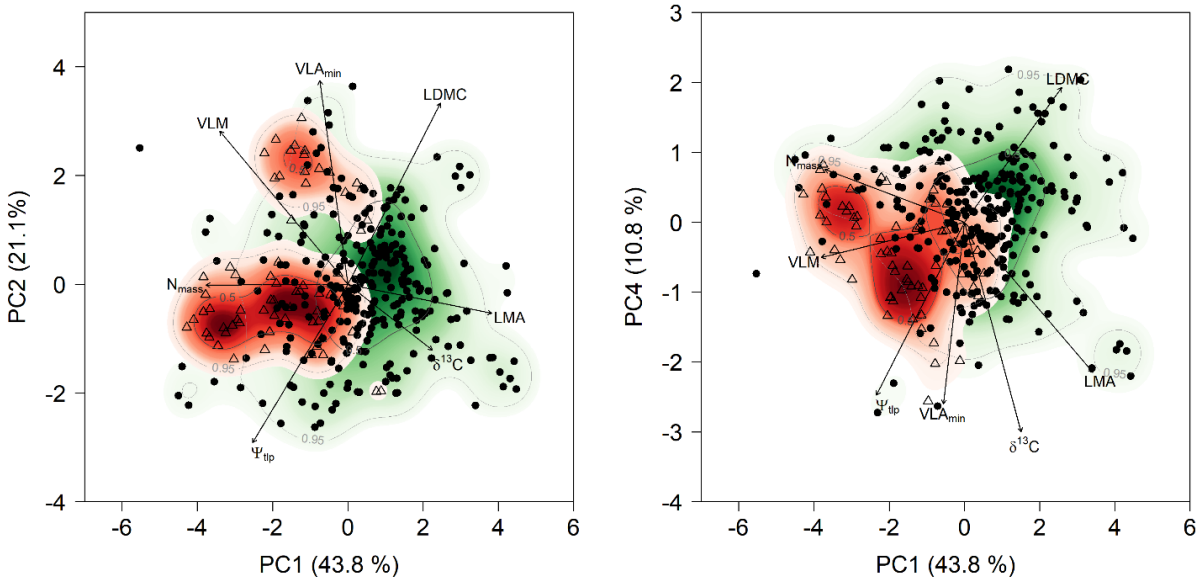

Fig. 5. PCA output computed on the correlation matrix of functional traits measured in IAS (empty triangles) and native species (solid circles). Solid arrows indicate direction and weighing of vectors representing the traits considered. The colour gradient indicates regions of highest occurrence probability of native species (green) and IAS (red) in the trait space defined by PC1, PC2 (left panel) and PC1 and PC4 (right panel), with contour lines indicating 0.5 and 0.95 quantiles distribution.

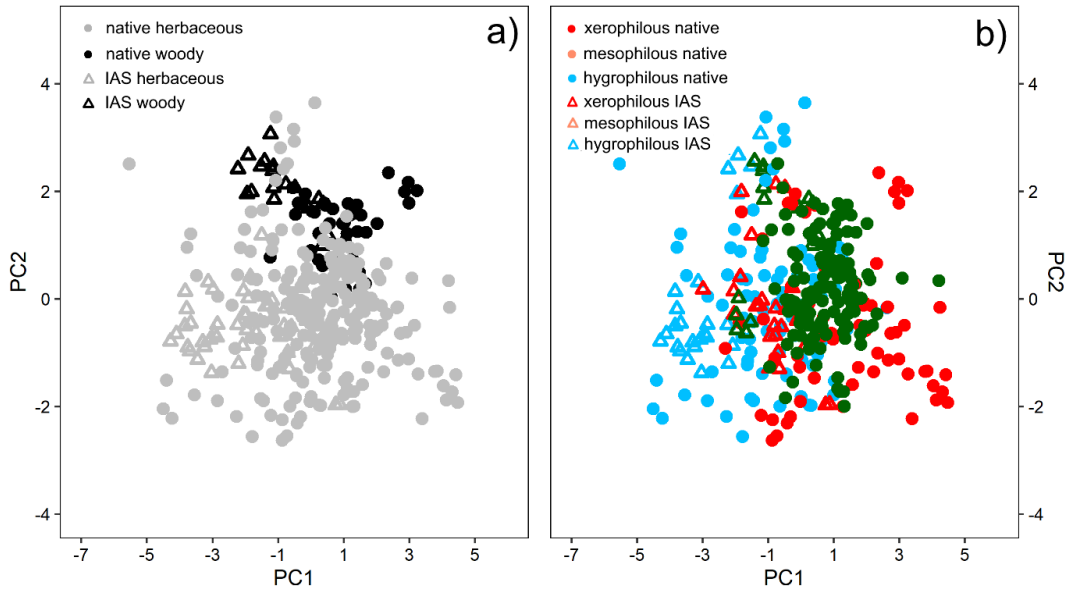

Fig. 6. PCA output computed on correlation matrix of functional traits measured in IAS (empty triangles) and native species (solid circles). a) different growth forms are overlaid on the ordination axes, b) different habitat types ordered along the water availability gradient are superimposed. Red colour indicates species occurring in xeric sites, green colour indicates those occurring in mesic sites and blue colour indicates species occurring in hydric sites.

4. DISCUSSION

4.1 IAS share lower drought resistance and denser venation network than natives

The recently described relationships between LES, HSE and vein traits have suggested that these traits are coordinated, and that their trade-offs might be useful to highlight the fundamental functions underlying the broader acquisitive-conservative continuum of terrestrial plant species (Díaz et al., 2016; Reich, 2014). Acquisitive species usually have lower leaf construction costs and higher productivity, due to high K_{stem} and K_{leaf}, that are coordinated in the HSE trade-off along with water relation parameters (e.g. Ψ_{tlp}) (Gleason et al., 2016; Nardini & Luglio, 2014). We showed that IAS had lower leaf construction costs (i.e. lower LMA) and higher π_0 and Ψ_{tlp} than native species (Fig. 1). IAS have been reported to be more impacted by drought than native species (Valliere et al., 2019), and this would be consistent with their higher Ψ_{tlp}. Under optimal water availability, IAS tend to grow faster than native species (Valliere et al., 2019), as a likely outcome of the trade-off between construction costs and water transport efficiency. We did not directly measure the hydraulic properties of stems or leaves, due to the time-consuming nature of such measurements considering the large number of individuals analysed in the present study. However, both VLA_{min} and VLM are mechanistically related to leaf hydraulic capacity (Scoffoni et al., 2016), as described in the "flux trait network" (Sack et al., 2013). IAS had higher values of VLA_{min} and VLM (Fig. 1), suggesting that they might have higher K_{leaf} and might thus be able to sustain higher transpiration rates. Higher VLA_{min} or VLM contribute to increasing K_{leaf} by providing more parallel water pathways, and by shortening the outside-xylem water pathway, thus reducing the resistance to water flow towards evaporative sites (Iida et al., 2016; McKown et al., 2010; Sack et al., 2013). We hypothesized that IAS could occupy the region of the HSE trade-off characterised by low drought resistance and high water transport efficiency, potentially explaining their ability to rapidly spread when introduced in exotic ranges. However, further studies directly measuring water transport efficiency (in terms of K_{leaf}) are required to support our hypothesis. Higher VLA_{min} or VLM are generally associated with higher gas exchange rates (Scoffoni et al., 2016). In this study, IAS had higher N_{mass} (a proxy of photosynthetic rates) than native species but similar $\delta^{13}C$, which is an integrated measurement of stomatal conductance (Dawson et al., 2002; Prieto et al., 2017), suggesting that they could have higher photosynthetic rates at any given stomatal conductance.

4.2 IAS and native species separated along the LES, HSE and vein traits trade-offs

Previous studies on plant invasions have provided contrasting evidence for differences in functional traits between native and invasive species (Díaz de León Guerrero et al., 2020; Funk & Zachary, 2010; Godoy et al., 2011; Hulme & Bernard-Verdier, 2018; Leffler et al., 2014;

van Kleunen et al., 2010). This uncertainty might arise from the different numbers of species included in each analysis, or from mixing traits measured in the field and in greenhouse experiments (Leffler et al., 2014), or could be due to the context-dependency nature of plant invasions (Funk, 2013; Funk & Vitousek, 2007). However, most of the previous comparisons between native and invasive species did not include traits mechanistically related to physiological functions ("mechanistic traits", *sensu* Brodribb, 2017; "process traits", *sensu* Volaire et al., 2020) or did not integrate different traits in specific trade-offs. We argued that measuring mechanistic traits coordinated in trade-offs would better depict which mechanisms underlie different growth strategies, and might be more useful to address ecological issues, such as the determination of plant functions favouring plant invasion. As proposed by Reich (2014), LES traits capture important trade-offs but only related to two key resources (carbon and nutrients), and the inclusion of traits related to water use and acquisition (the third key resource) might be useful to describe the functions underlying the acquisitive-conservative continuum.

In this light, given the differences between IAS and native species described above, we hypothesized that they occupy different positions along the trade-offs drawn by LES, HSE and vein traits. Fig. 2 showed the significant trade-offs between LMA and the other measured traits. While native species spread along these trade-offs, IAS tended to occupy the region associated with lower construction costs and higher Ψ_{tlp}, N_{mass} and VLM, but lower $\delta^{13}C$. These results suggested that the higher resistance to drought in native species comes at the expense of higher carbon investment, as leaves with higher LMA have larger cell size, greater number of mesophyll cell layers and higher cell mass densities (John et al., 2017). Leaves with higher LMA usually have lower K_{leaf} on a mass basis (Villagra et al., 2013), implying that high carbon investment, typical of conservative species, comes also at the cost of lower efficiency in water supply, reflecting a broader coordination between leaf economics and hydraulics (Sack et al., 2013; Villagra et al., 2013; Zhu et al., 2018). The positive relationship found between Ψ_{tlp} and VLM (Fig. 3) confirms this hypothesis, since vein length (both expressed per unit area o per unit mass) has a key role in determining hydraulic supply to leaf tissues (Sack et al., 2013). Native species and IAS separated along this trade-off, and IAS tended to occupy the region associated with lower drought resistance (higher Ψ_{tlp}) and potentially higher water transport efficiency (higher VLM). We are aware that scaling traits, such as vein length, on a mass basis would produce a negative relationship with LMA and LMA-related traits. However, as pointed out by Sack et al. (2013), this demonstrates that in leaves with higher LMA, less vein length is constructed per leaf mass investment, giving a mechanistic explanation of why K_{leaf} is reduced in leaves with high LMA. Moreover, one of the advantages of scaling traits on a mass basis, is that they are more directly related to the relative growth rate (RGR) (Sack et al., 2013). According to the "flux trait network", higher efficiency in water supply can sustain higher leaf

gas exchange rates and whole-plant growth, as VLM (as well as VLA_{min}) was positively associated with A_{mass} (Sack et al., 2013; Scoffoni et al., 2016). In our study, VLM was positively associated with N_{mass} (Fig. 4) and negatively with $\delta^{13}C$ (Fig. 4), which are proxies of photosynthetic and gas exchange rates, respectively. IAS tended to have higher VLM and N_{mass} than native species, while the two groups of species did not separate along the VLM-$\delta^{13}C$ trade-off. Cavaleri & Sack (2010) reported that invasive species have higher leaf-level water use, with higher stomatal conductance and photosynthetic rates, than native species. This may be attributed to the differences in venation architecture, as the higher VLM in IAS could result in higher water transport capacity, which in turn could assure prompt recovery of stomatal conductance and of photosynthetic rates when water is available.

Based on the above relationships, we hypothesized that HSE and vein traits might set an important axis of variation between IAS and native species. Our analysis seems to confirm the hypothesis, as IAS generally separated from natives along the PC1, PC2 and PC4 axes, occupying the region of the functional space defined by lower LMA and higher N_{mass}, VLA_{min}, VLM and Ψ_{tlp} values (Fig. 5). Notably, our data show that the consistency of this pattern is maintained through different growth forms and contrasting environmental conditions. Woody and herbaceous species were split along PC2 (Fig. 6a), and again PC1 determined the separation between woody IAS and woody natives. On the other hand, PC2 allowed to separate between herbaceous and woody IAS, which occupied the upper part of the functional space drawn by PC1 and PC2. When accounting for habitat types, IAS tended to occupy the same region of the functional space occupied by species growing in hydric sites (Fig. 6b), which typically have an acquisitive strategy. Curiously, we checked whether native species in our dataset are reported as alien within the GLoNAF database (van Kleunen et al., 2019), and we found that 16 native species were reported as alien elsewhere. 11 out of the 16 species were sampled in the hydric sites (see Tab. S5 in Appendix A) and this, combined with our previous results, strengthen the hypothesis that IAS might share a suite of traits reflecting functions that are generally associated with their invasiveness. This is further confirmed when comparing single traits where the differences between IAS and native species did not depend on site type or growth form (i.e. the interaction between status and site type and between status and growth form were not significant, see Appendix B).

Previous studies have suggested that trait divergence enhances the invasion success of alien species (Divíšek et al., 2018; Marchini et al., 2019; Tordoni et al., 2020), but the direction of traits differences was not consistent in all of them. Generally, IAS are taller than native species, with lower biomass invested in leaf construction and seed production (van Kleunen et al., 2010), but these differences might disappear when accounting for invasion stage and/or in multi-years analyses (Catford et al., 2019). In our analysis, the two groups of species seemed to be positioned along the “fast-slow economic spectrum” proposed by Reich

(2014), with IAS occupying the fast-growth region of the functional space. While this trend has been previously reported in previous studies (Barros et al., 2020; Díaz de León Guerrero et al., 2020; Pyšek & Richardson, 2008; Tordoni et al., 2020, 2019; van Kleunen et al., 2010), very few attempted to highlight the hydraulic basis of the fast growth and higher resource acquisition ability reported in IAS.

In conclusion, our data provide a mechanistic perspective for successful invasion in natural ecosystems. Here, we demonstrated that IAS tend to occupy the fast-growth region of the spectrum proposed by Reich et al. (2014), independently of site type or growth form. From a leaf-level perspective, hydraulic and vein traits provide stronger mechanistic linkages between construction costs and photosynthetic and growth rates and suggest that HSE-related traits possibly play a central role in determining the invasive potential of IAS. Specifically, IAS could reduce costs associated with leaf construction and resistance to drought stress having, at the same time, high efficiency of water transport and photosynthetic rates by developing a denser venation network, translating in higher growth rates than native and more conservative species. These findings might have important implications for predicting IAS success or failure under climate change scenarios especially in drought-prone ecosystems, such as those in the Mediterranean region.

REFERENCES

Anderson, M.J. (2001). A new method for non-parametric multivariate analysis of variance. *Austral Ecology*, 26, 32–46. doi: https://doi.org/10.1111/j.1442-9993.2001.01070.pp.x

Antunes, C., Pereira, A. J., Fernandes, P., Ramos, M., Ascensão, L., Correia, O., & Máguas, C. (2018). Understanding plant drought resistance in a Mediterranean coastal sand dune ecosystem: Differences between native and exotic invasive species. *Journal of Plant Ecology*, 11(1), 26–38. doi: 10.1093/jpe/rtx014

Barros, V., Melo, A., Santos, M., Nogueira, L., Frosi, G., & Santos, M. G. (2020). Different resource-use strategies of invasive and native woody species from a seasonally dry tropical forest under drought stress and recovery. *Plant Physiology and Biochemistry*, 147, 181–190. doi: 10.1016/j.plaphy.2019.12.018

Bartlett, M. K., Zhang, Y., Yang, J., Kreidler, N., Sun, S.-W., Lin, L., … Sack, L. (2016). Drought tolerance as a driver of tropical forest assembly: Resolving spatial signatures for multiple processes. *Ecology*, 97(2), 503–514. doi: https://doi.org/10.1890/15-0468.1

Bartlett, K., Scoffoni, C., & Sack, L. (2012a). The determinants of leaf turgor loss point and prediction of drought tolerance of species and biomes: A global meta-analysis. *Ecology Letters*, 15(5), 393–405. doi: 10.1111/j.1461-0248.2012.01751.x

Bartlett, M. K., Scoffoni, C., Ardy, R., Zhang, Y., Sun, S., Cao, K., & Sack, L. (2012b). Rapid determination of comparative drought tolerance traits: Using an osmometer to predict turgor loss point. *Methods in Ecology and Evolution*, 3(5), 880–888. doi: 10.1111/j.2041-210X.2012.00230.x

Barton, K. (2020). MuMIn: Multi-Model Inference. R package version 1.43.17.

Bates, D., Maechler, M., Bolker, B., Walker, S. (2015). Fitting Linear Mixed-Effects Models Using lme4. *Journal of Statistical Software*, 67(1), 1-48. doi:10.18637/jss.v067.i01.

Brodribb, T. J. (2009). Xylem hydraulic physiology: The functional backbone of terrestrial plant productivity. *Plant Science*, 177(4), 245–251. doi: 10.1016/j.plantsci.2009.06.001

Brodribb, T. J. (2017). Progressing from 'functional' to mechanistic traits. *New Phytologist*, 215(1), 9–11. doi: https://doi.org/10.1111/nph.14620

Bühler, J., Rishmawi, L., Pflugfelder, D., Huber, G., Scharr, H., Hülskamp, M., … Jahnke, S. (2015). phenoVein—A tool for leaf vein segmentation and analysis. *Plant Physiology*, 169(4), 2359-2370. doi: 10.1104/pp.15.00974

Catford, J. A., Smith, A. L., Wragg, P. D., Clark, A. T., Kosmala, M., Cavender-Bares, J., … Tilman, D. (2019). Traits linked with species invasiveness and community invasibility vary with time, stage and indicator of invasion in a long-term grassland experiment. *Ecology Letters*, 22(4), 593–604. doi: 10.1111/ele.13220

Cavaleri, M. A., Ostertag, R., Cordell, S., & Sack, L. (2014). Native trees show conservative water use relative to invasive trees: Results from a removal experiment in a Hawaiian wet forest. *Conservation Physiology*, 2(1), cou016–cou016. doi: 10.1093/conphys/cou016

Cavaleri, M. A., & Sack, L. (2010). Comparative water use of native and invasive plants at multiple scales: A global meta-analysis. *Ecology*, 91(9), 2705–2715. doi: 10.1890/09-0582.1

Crous, C. J., Jacobs, S. M., & Esler, K. J. (2012). Drought-tolerance of an invasive alien tree, *Acacia mearnsii* and two native competitors in fynbos riparian ecotones. *Biological Invasions*, 14(3), 619–631. doi: 10.1007/s10530-011-0103-y

Dawson, T. E., Mambelli, S., Plamboeck, A. H., Templer, P. H., & Tu, K. P. (2002). Stable Isotopes in Plant Ecology. *Annual Review of Ecology and Systematics*, 33(1), 507–559. doi: 10.1146/annurev.ecolsys.33.020602.095451

Díaz de León Guerrero, S. D., González-Rebeles Guerrero, G., Ibarra-Montes, T. M., Rodríguez Bastarrachea, A., Santos Cobos, R., Bullock, S. H., … Méndez-Alonzo, R. (2020). Functional traits indicate faster resource acquisition for alien herbs than native shrubs in an urban Mediterranean shrubland. *Biological Invasions*. doi: 10.1007/s10530-020-02290-w

Díaz, S., Kattge, J., Cornelissen, J. H. C., Wright, I. J., Lavorel, S., Dray, S., … Gorné, L. D. (2016). The global spectrum of plant form and function. *Nature*, 529(7585), 167–171. doi: 10.1038/nature16489

Divíšek, J., Chytrý, M., Beckage, B., Gotelli, N. J., Lososová, Z., Pyšek, P., … Molofsky, J. (2018). Similarity of introduced plant species to native ones facilitates naturalization, but differences enhance invasion success. *Nature Communications*, 9(1). doi: 10.1038/s41467-018-06995-4

Dray, S. (2008). On the number of principal components: A test of dimensionality based on measurements of similarity between matrices. *Computational Statistics & Data Analysis*, 52(4), 2228–2237. doi: 10.1016/j.csda.2007.07.015

Fan, Z.-X., Zhang, S.-B., Hao, G.-Y., Ferry Slik, J. and Cao, K.-F. (2012). Hydraulic conductivity traits predict growth rates and adult stature of 40 Asian tropical tree species better than wood density. *Journal of Ecology*, 100, 732-741. https://doi.org/10.1111/j.1365-2745.2011.01939.x

Funk, J. L. (2013). The physiology of invasive plants in low-resource environments. *Conservation Physiology*, 1(1), cot026–cot026. doi: 10.1093/conphys/cot026

Funk, J. L., Standish, R. J., Stock, W. D., Valladares, F. (2016). Plant functional traits of dominant native and invasive species in mediterranean- climate ecosystems. Ecology, 97(1), 75-83. doi: 10.1890/15-0974.1

Funk, J. L., & Vitousek, P. M. (2007). Resource-use efficiency and plant invasion in low-resource systems. *Nature*, 446(7139), 1079–1081. doi: 10.1038/nature05719

Funk, J. L., & Zachary, V. A. (2010). Physiological responses to short-term water and light stress in native and invasive plant species in southern California. *Biological Invasions*, 12(6), 1685–1694. doi: 10.1007/s10530-009-9581-6

Galasso, G., Conti, F., Peruzzi, L., Ardenghi, N. M. G., Banfi, E., Celesti-Grapow, L., … Bartolucci, F. (2018). An updated checklist of the vascular flora alien to Italy. *Plant Biosystems - An International Journal Dealing with All Aspects of Plant Biology*, 152(3), 556–592. doi: 10.1080/11263504.2018.1441197

Gleason, S. M., Westoby, M., Jansen, S., Choat, B., Hacke, U. G., Pratt, R. B., … Zanne, A. E. (2016). Weak tradeoff between xylem safety and xylem-specific hydraulic efficiency across the world's woody plant species. *New Phytologist*, 209(1), 123–136. doi: 10.1111/nph.13646

Godoy, O., de Lemos-Filho, J. P., & Valladares, F. (2011). Invasive species can handle higher leaf temperature under water stress than Mediterranean natives. *Environmental and Experimental Botany*, 71(2), 207–214. doi: 10.1016/j.envexpbot.2010.12.001

Griffin-Nolan, R.J., Ocheltree, T.W., Mueller, K.E., Blumenthal, D.M., Kray, J.A., Knapp, A.K. (2019). Extending the osmometer method for assessing drought tolerance in herbaceous species. *Oecologia*, 189, 353-363, doi: https://doi.org/10.1007/s00442-019-04336-wHacke, U. G., Spicer, R., Schreiber, S. G., & Plavcová, L. (2017). An ecophysiological and developmental perspective on variation in vessel diameter. *Plant, Cell & Environment*, 40(6), 831–845. doi: https://doi.org/10.1111/pce.12777

Hulme, P. E. (2011). Addressing the threat to biodiversity from botanic gardens. *Trends in Ecology & Evolution*, 26(4), 168–174. doi: 10.1016/j.tree.2011.01.005

Hulme, P. E., & Bernard-Verdier, M. (2018). Comparing traits of native and alien plants: Can we do better? *Functional Ecology*, 32, 117–125. doi: 10.1111/1365-2435.12982

Iida, Y., Sun, I.-F., Price, C. A., Chen, C.-T., Chen, Z.-S., Chiang, J.-M., … Swenson, N. G. (2016). Linking leaf veins to growth and mortality rates: An example from a subtropical tree community. *Ecology and Evolution*, 6(17), 6085–6096. doi: 10.1002/ece3.2311

John, G. P., Scoffoni, C., Buckley, T. N., Villar, R., Poorter, H., & Sack, L. (2017). The anatomical and compositional basis of leaf mass per area. *Ecology Letters*, 20(4), 412–425. doi: 10.1111/ele.12739

Larter, M., Pfautsch, S., Domec, J.-C., Trueba, S., Nagalingum, N., & Delzon, S. (2017). Aridity drove the evolution of extreme embolism resistance and the radiation of conifer genus *Callitris*. *New Phytologist*, 215(1), 97–112. doi: 10.1111/nph.14545

Leffler, A. J., James, J. J., Monaco, T. A., & Sheley, R. L. (2014). A new perspective on trait differences between native and invasive exotic plants. *Ecology*, *95*(2), 298–305. doi: 10.1890/13-0102.1

Leishman, M. R., Cooke, J., Richardson, D. M., & Newman, J. (2014). Evidence for shifts to faster growth strategies in the new ranges of invasive alien plants. *Journal of Ecology*, 102(6), 1451–1461. doi: 10.1111/1365-2745.12318

Leishman, M. R., Haslehurst, T., Ares, A., & Baruch, Z. (2007). Leaf trait relationships of native and invasive plants: Community- and global-scale comparisons. *New Phytologist*, 176(3), 635–643. doi: 10.1111/j.1469-8137.2007.02189.x

Lenz, T. I., Wright, I. J., & Westoby, M. (2006). Interrelations among pressure-volume curve traits across species and water availability gradients. *Physiologia Plantarum*, 127(3), 423–433. doi: 10.1111/j.1399-3054.2006.00680.x

Marchini, G. L., Maraist, C. A., & Cruzan, M. B. (2019). Trait divergence, not plasticity, determines the success of a newly invasive plant. *Annals of Botany*, 123(4), 667–679. doi: 10.1093/aob/mcy200

McKown, A. D., Cochard, H., & Sack, L. (2010). Decoding Leaf Hydraulics with a Spatially Explicit Model: Principles of Venation Architecture and Implications for Its Evolution. *The American Naturalist*, 175(4), 447–460. doi: 10.1086/650721

Nardini, A., Petruzzellis, F., Marusig, D., Tomasella, M., Natale, S., Altobelli, A., Calligaris, C., Floriddia, G., Cucchi, F., Forte, E., Zini, L. (2021), Water 'on the rocks': a summer drink for thirsty trees?. *New Phytologist*, 229, 199-212. https://doi.org/10.1111/nph.16859

Nardini, A., & Luglio, J. (2014). Leaf hydraulic capacity and drought vulnerability: Possible trade-offs and correlations with climate across three major biomes. *Functional Ecology*, 28(4), 810–818. doi: 10.1111/1365-2435.12246

Ocheltree, T.W., Nippert, J.B., Vara Prasad, P.V. (2016). A safety vs efficiency trade-off identified in the hydraulic pathway of grass leaves is decoupled from photosynthesis, stomatal conductance and precipitation. *New Phytologist*, 210: 97-107. doi: 10.1111/nph.13781

Oksanen, J., Blanchet, G.F., Friendly, M., Kindt, R., Legendre, P., McGlinn, D., Minchin, P.R., O'Hara, R.B., Simpson, G.L., Solymos, P., Stevens, M.H.H., Szoecs, E., Wagner, H. (2017). Vegan: community ecology package. R package version 2.4.3

Onoda, Y., Wright, I. J., Evans, J. R., Hikosaka, K., Kitajima, K., Niinemets, Ü., … Westoby, M. (2017). Physiological and structural tradeoffs underlying the leaf economics spectrum. *New Phytologist*, 214(4), 1447–1463. doi: 10.1111/nph.14496

Penuelas, J., Sardans, J., Llusià, J., Owen, S. M., Carnicer, J., Giambelluca, T. W., … Niinemets, Ü. (2009). Faster returns on 'leaf economics' and different biogeochemical

niche in invasive compared with native plant species. *Global Change Biology*, 16(8), 2171–2185. doi: 10.1111/j.1365-2486.2009.02054.x

Petruzzellis, F., Nardini, A., Savi, T., Tonet, V., Castello, M., & Bacaro, G. (2019). Less safety for more efficiency: Water relations and hydraulics of the invasive tree *Ailanthus altissima* (Mill.) Swingle compared with native *Fraxinus ornus* L. *Tree Physiology,* 39(1), 76-87. doi: 10.1093/treephys/tpy076

Petruzzellis, F., Palandrani, C., Savi, T., Alberti, R., Nardini, A., & Bacaro, G. (2017). Sampling intraspecific variability in leaf functional traits: Practical suggestions to maximize collected information. *Ecology and Evolution*, 7(24), 11236–11245. doi: 10.1002/ece3.3617

Petruzzellis, F., Savi, T., Bacaro, G., & Nardini, A. (2019). A simplified framework for fast and reliable measurement of leaf turgor loss point. *Plant Physiology and Biochemistry*, 139, 395–399. doi: 10.1016/j.plaphy.2019.03.043

Pinheiro, J., Bates, D., DebRoy, S., Sarkar, D. (2020). nlme: Linear and Nonlinear Mixed Effects Models. R package version 3.1-151, https://CRAN.R-project.org/package=nlme.

Pintó-Marijuan, M., & Munné-Bosch, S. (2013). Ecophysiology of invasive plants: Osmotic adjustment and antioxidants. *Trends in Plant Science*, 18(12), 660–666. doi: 10.1016/j.tplants.2013.08.006

Poldini, L. (1989). *La vegetazione del Carso isontino e triestino.* Trieste: Lint.

Poldini, L., Gioitti, G., Martini, F., & Budin, S. (1992). *Introduzione alla flora e alla vegetazione del Carso*. Trieste: Lint.

Poorter H., Niinemets, Ü., Poorter., L., Wright, I.J., Villar, R. (2009). Causes and consequences of variation in leaf mass per area (LMA): a meta-analysis. New Phytologist, 182, 565-588. doi: https://doi.org/10.1111/j.1469-8137.2009.02830.x

Prieto, I., Querejeta, J. I., Segrestin, J., Volaire, F., & Roumet, C. (2018). Leaf carbon and oxygen isotopes are coordinated with the leaf economics spectrum in Mediterranean rangeland species. *Functional Ecology,* 32, 612-625. doi: 10.1111/1365-2435.13025

Pyšek, P., & Richardson, D. M. (2008). Traits associated with invasiveness in alien plants: Where do we stand? In D. W. Nentwig (Ed.), *Biological Invasions* (pp. 97–125). Springer Berlin Heidelberg. doi: 10.1111/j.1365-2699.2006.01578.x

Reich, P. B. (2014). The world-wide 'fast-slow' plant economics spectrum: A traits manifesto. *Journal of Ecology*, 102(2), 275–301. doi: 10.1111/1365-2745.12211

Richardson, D. M., Py, P., Rejmánek, M., Barbour, M. G., Panetta, F. D., & West, C. J. (2000). Naturalization and invasion of alien plants: Concepts and definitions. *Diversity and Distributions*, 6, 93-107. doi: https://doi.org/10.1046/j.1472-4642.2000.00083.x

Sack, L., Scoffoni, C., John, G. P., Poorter, H., Mason, C. M., Mendez-Alonzo, R., & Donovan, L. A. (2013). How do leaf veins influence the worldwide leaf economic spectrum? Review and synthesis. *Journal of Experimental Botany*, 64(13), 4053–4080. doi: 10.1093/jxb/ert316

Schneider, C. A., Rasband, W. S., & Eliceiri, K. W. (2012). NIH Image to ImageJ: 25 years of image analysis. *Nature Methods*, 9(7), 671–675. doi: 10.1038/nmeth.2089

Scoffoni, C., Chatelet, D. S., Pasquet-kok, J., Rawls, M., Donoghue, M. J., Edwards, E. J., & Sack, L. (2016). Hydraulic basis for the evolution of photosynthetic productivity. *Nature Plants*, 2, 16072. doi: 10.1038/nplants.2016.72

Tordoni, E., Petruzzellis, F., Nardini, A., & Bacaro, G. (2020). Functional Divergence Drives Invasibility of Plant Communities at the Edges of a Resource Availability Gradient. *Diversity*, 12(4), 148.

Tordoni, E., Petruzzellis, F., Nardini, A., Savi, T., & Bacaro, G. (2019). Make it simpler: Alien species decrease functional diversity of coastal plant communities. *Journal of Vegetation Science*, 30, 498-509. doi: 10.3390/d12040148

Urbanc J, Mezga K, Zini L. 2012. An assessment of capacity of Brestovica –Klariči Karst water supply (Slovenia). *Acta Carsologica* 41: 89–100.

Valliere, J. M., Escobedo, E. B., Bucciarelli, G. M., Sharifi, M. R., & Rundel, P. W. (2019). Invasive annuals respond more negatively to drought than native species. *New Phytologist*, 223(3), 1647–1656. doi: 10.1111/nph.15865

van Kleunen, M., Pyšek, P., Dawson, W., Essl, F., Kreft, H., Pergl, J., … Winter, M.. (2019). The Global Naturalized Alien Flora (GloNAF) database. *Ecology,* 100:e02542. doi: 10.1002/ecy.2542

van Kleunen, M., Weber, E., & Fischer, M. (2010). A meta-analysis of trait differences between invasive and non-invasive plant species. *Ecology Letters*, 13(2), 235–245. doi: 10.1111/j.1461-0248.2009.01418.x

Vasquez-Valderrama, M., González-M, R., López-Camacho, R., Baptiste, M. P., & Salgado-Negret, B. (2020). Impact of invasive species on soil hydraulic properties: Importance of functional traits. *Biological Invasions*. doi: 10.1007/s10530-020-02222-8

Venables, W. N., Ripley, B. D. (2002). Modern Applied Statistics with S. Springer.

Villagra, M., Campanello, P. I., Bucci, S. J., & Goldstein, G. (2013). Functional relationships between leaf hydraulics and leaf economic traits in response to nutrient addition in subtropical tree species. *Tree Physiology*, 33(12), 1308–1318. doi: 10.1093/treephys/tpt098

Volaire, F., Gleason, S.M., Delzon, S. (2020). What do you mean “functional” in ecology? Patterns versus processes. Ecology and Evolution, 10, 11875-11885. doi: https://doi.org/10.1002/ece3.6781

Wickham, H. (2016). ggplot2: Elegant Graphics for Data Analysis. Springer-Verlag New York. Retrieved from https://ggplot2.tidyverse.org

Wright, I. J., Reich, P. B., Westoby, M., Ackerly, D. D., Baruch, Z., Bongers, F., … Diemer, M. (2004). The worldwide leaf economics spectrum. *Nature*, 428(6985), 821–827. doi: https://doi.org/10.1038/nature02403

Yazaki, K., Sano, Y., Fujikawa, S., Nakano, T., & Ishida, A. (2010). Response to dehydration and irrigation in invasive and native saplings: Osmotic adjustment versus leaf shedding. *Tree Physiology*, 30(5), 597–607. doi: 10.1093/treephys/tpq010

Zeballos, S. R., Giorgis, M. A., Cingolani, A. M., Cabido, M., Whitworth-Hulse, J. I., & Gurvich, D. E. (2014). Do alien and native tree species from Central Argentina differ in their water transport strategy? *Austral Ecology*, 39(8), 984–991. doi: 10.1111/aec.12171

Zhang, J.-L. and Cao, K.-F. (2009). Stem hydraulics mediates leaf water status, carbon gain, nutrient use efficiencies and plant growth rates across dipterocarp species. *Functional Ecology*, 23, 658-667. https://doi.org/10.1111/j.1365-2435.2009.01552.x

Zhu, S.-D., Chen, Y.-J., Ye, Q., He, P.-C., Liu, H., Li, R.-H., … Cao, K.-F. (2018). Leaf turgor loss point is correlated with drought tolerance and leaf carbon economics traits. *Tree Physiology*, 38(5), 658–663. doi: 10.1093/treephys/tpy013

Appendix A

Fig. S1 Map of the study area with respect to Italian peninsula, right inset shows the location of sampling sites.

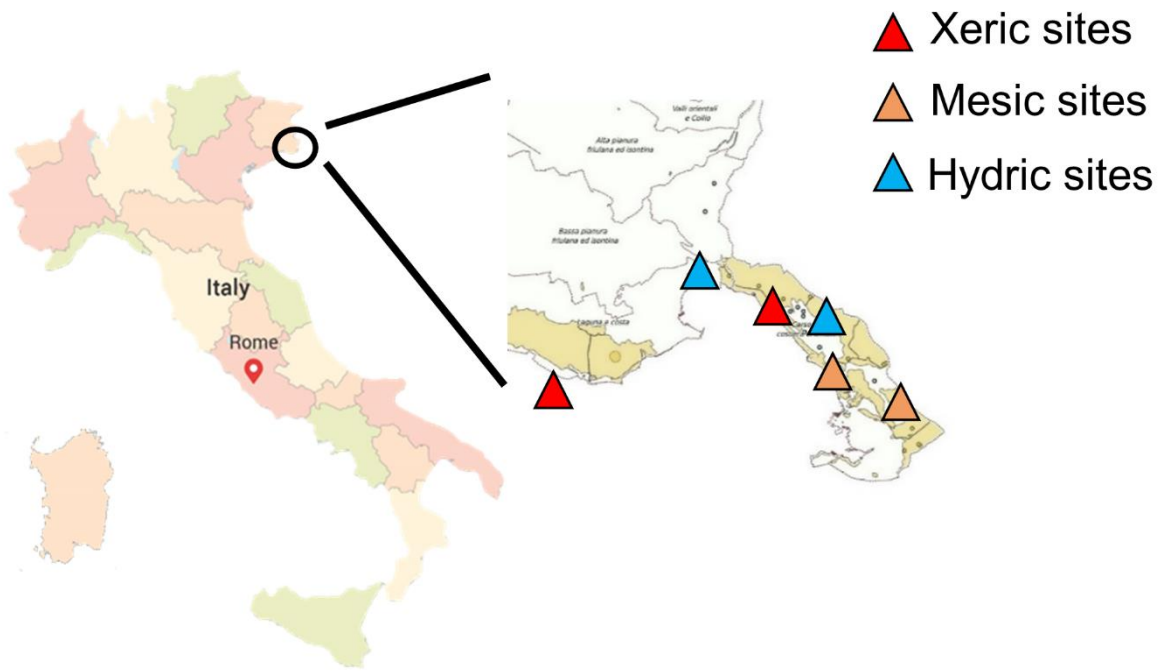

Fig. S2 Example of vegetation present in the sampling sites.

Hydric sites

1

2

Mesic sites

3

4

Xeric sites

5

6

.

Fig. S3 PCA output computed on the correlation matrix of functional traits measured in IAS (empty triangles) and native species (solid circles). Solid arrows indicate direction and weighing of vectors representing the traits considered. The colour gradient indicates regions of highest occurrence probability of native species (green) and IAS (red) in the trait space defined by PC1 and PC3, with contour lines indicating 0.5 and 0.95 quantiles distribution.

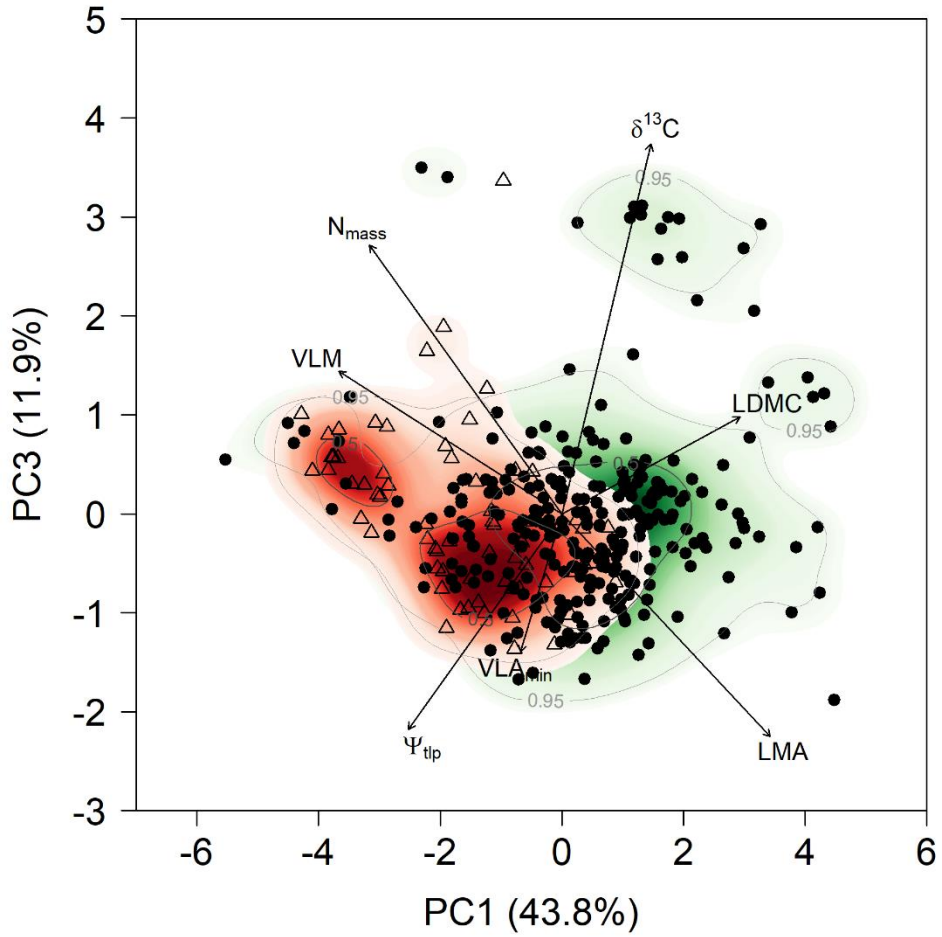

Tab. S1. Mean annual temperature (T, °C), mean annual precipitation (mm), consecutive dry days with precipitation < 5 mm (CDD) and number of days with precipitation > 1mm retrieved from the three whether stations (Lignano, Cervignano and Sgonico) closest to sampled sites. Data were downloaded from www.osmer.fvg.it. Reference period: 1992–2017.

	Hydric sites	**Mesic sites**	**Xeric sites**
Mean annual T, °C	13.6 ± 0.7	13.1 ± 0.6	15.2 ± 0.6
Mean annual precipitation, mm	1368 ± 285	1387 ± 293	999 ± 318
CDD	35 ± 11	34 ± 9	38 ± 9
N days with precipitation > 1mm	99 ± 19	102 ± 17	84 ± 16

Tab. S2 (provided in excel format) Mean values and standard deviation of the different functional traits recorded for each species.

Tab. S3 Spearman's coefficient (ρ) calculated on the traits measured in this study. *** = $p < 0.001$, ** = $p < 0.01$, * = $p < 0.05$, n.s. = $p > 0.05$.

	LMA	**LDMC**	**π_0**	**Ψ_{tlp}**	**VLA_{min}**	**VLM**	**N_{mass}**
LDMC	0.40***						
π_0	-0.36***	-0.73***					
Ψ_{tlp}	-0.35***	-0.73***	0.99***				
VLA_{min}	$-0.11^{n.s.}$	0.19***	$-0.09^{n.s}$	$-0.09^{n.s}$			
VLM	-0.63***	-0.24***	0.28**	0.28***	0.49***		
N_{mass}	-0.67***	-0.38***	0.28***	0.27***	$-0.08^{n.s}$	0.59***	
$\delta^{13}C$	0.59***	0.45***.	-0.41***	-0.41**	$0.07^{n.s}$	-0.49***	-0.40***

Tab. S4. Results of PERMANOVA analysis testing for the effect of Status (IAS vs native), growth form (woody vs herbaceous) and Site type (hydric, mesic and xeric). df, degrees of freedom; SS, sum of squares, MS, mean squares; Pseudo-F: pseudo-Fstatistic.

	df	SS	MS	Pseudo-F	R^2	p-value
Status	1	224.23	244.23	38.67	0.10	0.001
Residuals	347	2191.77	6.32		0.90	
Total	348	2436.00				
Growth form	1	194.80	194.80	30.16	0.08	0.001
Residuals	347	2241.20	6.46		0.92	
Total	348	2436.00				
Site type	1	435.58	217.79	37.67	0.18	0.001
Residuals	347	2000.42	5.78		0.82	
Total	348	2436.00				

Tab S5. List of native species in out dataset reported as alien in GLoNAF database.

Species	Site type
Agrostis stolonifera	Hydric
Ammophila arenaria	Xeric
Cynodon dactylon	Xeric
Hedera helix	Hydric
Leersia oryzoides	Hydric
Lythrum salicaria	Hydric
Mentha arvensis	Hydric
Persicaria hydropiper	Hydric
Phragmites australis	Hydric
Plantago major	Hydric
Populus nigra	Hydric
Quercus ilex	Xeric
Ranunculus repens	Hydric
Silene vulgaris	Xeric
Trifolium rubens	Mesic

Appendix B

Hereafter, we report the outputs of the linear mixed models run to assess trait differences between IAS and native species (see Materials and Methods for details). SD = standard deviation; SE = standard error; df = degrees of freedom. Please note that estimate parameters of models with log-transformed response variables are presented in log scale.

LMA (log transformed)

Random effect

Groups	Name	Variance	SD
Species	Intercept	0.09	0.30
Residual		0.05	0.22

Number of observations: 349. Groups: Species = 95

Fixed effect parameters estimates

	Estimate	SE	df	t-value	p-value
Intercept	1.10	0.14	85.88	7.94	< 0.001
Status -native	0.36	0.15	89.10	2.35	0.02
Site type -mesic	0.65	0.24	70.48	3.70	0.001
Site type -xeric	0.60	0.18	95.85	3.22	0.002
Growth form - woody	0.22	0.20	69.42	1.11	0.27
Status -native: Site type -mesic	0.01	0.25	74.57	0.03	0.61
Status -native: Site type -xeric	0.05	0.20	98.01	0.25	0.83
Status -native: Growth form - woody	-0.07	0.21	78.53	-0.36	0.72

Anova table

	F-value	df	p-value
Intercept	1280.62	74.97	< 0.001
Status	11.65	78.31	0.001
Site type	22.21	82.59	< 0.001
Growth form	3.01	77.38	0.09
Status*Site type	0.03	81.77	0.97
Status*Growth form	0.13	76.99	0.72
R^2 marginal	0.46		
R^2 conditional	0.81		

LDMC (log transformed)

Random effect

Groups	Name	Variance	SD
Species	Intercept	0.12	0.35
Residual		0.02	0.12

Number of observations: 349. Groups: Species = 95

Fixed effect parameters estimates

	Estimate	SE	df	t-value	p-value
Intercept	5.32	0.14	81.25	37.13	< 0.001
Status -native	0.27	0.16	83.85	1.74	0.09
Site type -mesic	-0.11	0.26	76.08	-0.41	0.68
Site type -xeric	0.09	0.18	102.31	0.51	0.61
Growth form - woody	0.67	0.21	76.68	3.14	0.002
Status -native: Site type -mesic	0.37	0.27	79.60	1.39	0.17
Status -native: Site type -xeric	-0.07	0.20	104.20	-0.36	0.72
Status -native: Growth form - woody	-0.57	0.23	85.53	-2.53	0.01

Anova table

	F-value	df	p-value
Intercept	11189.85	85.95	< 0.001
Status	0.65	92.33	0.42
Site type	0.23	93.90	0.79
Growth form	11.55	89.52	0.001
Status*Site type	1.41	93.14	0.25
Status*Growth form	6.37	88.34	0.01
R^2 marginal	0.24		
R^2 conditional	0.91		

π_0 (log transformed absolute values)

Random effect

Groups	Name	Variance	SD
Species	Intercept	0.09	0.29
Residual		0.02	0.13

Number of observations: 349. Groups: Species = 95

Fixed effect parameters estimates

	Estimate	SE	df	t-value	p-value
Intercept	-0.29	0.12	79.59	-2.41	0.02
Status -native	0.39	0.13	82.57	3.03	0.003
Site type -mesic	0.20	0.24	72.59	0.83	0.41
Site type -xeric	0.40	0.15	101.12	2.65	0.09
Growth form - woody	0.43	0.21	70.83	2.10	0.04
Status -native: Site type -mesic	-0.07	0.24	75.56	-0.30	0.76
Status -native: Site type -xeric	-0.02	0.17	102.93	-0.15	0.88
Status -native: Growth form - woody	-0.30	0.21	75.20	-1.41	0.16

Anova table

	F-value	df	p-value
Intercept	24.81	81.17	< 0.001
Status	5.31	83.91	0.02
Site type	11.40	95.47	< 0.001
Growth form	7.26	84.11	0.009
Status*Site type	0.04	94.55	0.96
Status*Growth form	1.99	83.47	0.16
R^2 marginal	0.30		
R^2 conditional	0.85		

Ψ_{tlp} (log transformed absolute values)

Random effect

Groups	Name	Variance	SD
Species	Intercept	0.08	0.29
Residual		0.02	0.12

Number of observations: 349. Groups: Species = 95

Fixed effect parameters estimates

	Estimate	SE	df	t-value	p-value
Intercept	0.01	0.12	79.51	0.12	0.91
Status -native	0.38	0.13	82.46	3.04	0.003
Site type -mesic	0.18	0.23	72.41	0.81	0.42
Site type -xeric	0.38	0.15	100.82	2.62	0.01
Growth form - woody	0.43	0.20	70.59	2.13	0.04
Status -native: Site type -mesic	-0.07	0.23	75.37	-0.28	0.78
Status -native: Site type -xeric	-0.03	0.16	102.57	-0.19	0.85
Status -native: Growth form - woody	-0.29	0.20	74.99	-1.44	0.15

Anova table

	F-value	df	p-value
Intercept	133.79	81.04	< 0.001
Status	5.21	83.76	0.02
Site type	10.96	95.25	< 0.001
Growth form	7.50	83.96	0.008
Status*Site type	0.04	94.33	0.96
Status*Growth form	2.06	83.32	0.16
R^2 marginal	0.30		
R^2 conditional	0.86		

VLA_{min}

Random effect

Groups	Name	Variance	SD
Species	Intercept	4.80	2.19
Residual		2.26	1.50

Number of observations: 349. Groups: Species = 95

Fixed effect parameters estimates

	Estimate	SE	df	t-value	p-value
Intercept	7.96	0.94	75.48	8.45	< 0.001
Status -native	-1.17	1.03	78.37	-1.14	0.26
Site type -mesic	1.89	1.65	63.02	1.15	0.25
Site type -xeric	0.61	1.19	86.47	0.51	0.61
Growth form - woody	4.19	1.36	62.33	3.08	0.003
Status -native: Site type -mesic	-0.70	1.72	66.67	-0.40	0.69
Status -native: Site type -xeric	-0.58	1.34	88.31	-0.43	0.67
Status -native: Growth form - woody	-0.04	1.42	70.26	-0.03	0.98

Anova table

	F-value	df	p-value
Intercept	875.89	76.56	< 0.001
Status	5.78	80.37	0.02
Site type	1.64	84.57	0.20
Growth form	34.06	79.05	< 0.001
Status*Site type	0.13	83.73	0.88
Status*Growth form	0.01	78.57	0.98
R^2 marginal	0.49		
R^2 conditional	0.84		

VLM (log transformed)

Random effect

Groups	Name	Variance	SD
Species	Intercept	0.22	0.47
Residual		0.07	0.27

Number of observations: 349. Groups: Species = 95

Fixed effect parameters estimates

	Estimate	SE	df	t-value	p-value
Intercept	5.56	0.21	83.20	26.13	< 0.001
Status -native	-0.55	0.23	86.99	-2.41	0.02
Site type -mesic	-0.46	0.38	72.94	-1.21	0.23
Site type -xeric	-0.52	0.26	100.79	-1.96	0.05
Growth form - woody	0.19	0.31	72.92	0.61	0.55
Status -native: Site type -mesic	-0.07	0.39	77.05	-0.19	0.85
Status -native: Site type -xeric	-0.05	0.30	103.47	-0.17	0.87
Status -native: Growth form - woody	0.29	0.32	80.59	0.89	0.37

Anova table

	F-value	df	p-value
Intercept	4336.28	81.00	< 0.001
Status	8.83	86.03	0.004
Site type	7.28	90.85	0.001
Growth form	4.26	83.41	0.04
Status*Site type	0.02	89.94	0.98
Status*Growth form	0.80	82.80	0.37
R^2 marginal	0.33		
R^2 conditional	0.84		

N_{mass}

Random effect

Groups	Name	Variance	SD
Species	Intercept	0.29	0.54
Residual		0.25	0.50

Number of observations: 296. Groups: Species = 94

Fixed effect parameters estimates

	Estimate	SE	df	t-value	p-value
Intercept	3.94	0.27	67.32	14.78	< 0.001
Status -native	-1.27	0.29	69.76	-4.32	< 0.001
Site type -mesic	-1.76	0.47	60.70	-3.73	< 0.001
Site type -xeric	-1.62	0.34	72.96	-4.74	< 0.001
Growth form - woody	0.24	0.39	59.09	0.64	0.52
Status -native: Site type -mesic	0.91	0.50	64.04	1.84	0.07
Status -native: Site type -xeric	0.77	0.39	74.88	1.98	0.05
Status -native: Growth form - woody	-0.13	0.43	67.89	-0.30	0.77

Anova table

	F-value	df	p-value
Intercept	650.48	75.00	< 0.001
Status	15.01	77.40	< 0.001
Site type	24.58	79.59	< 0.001
Growth form	0.76	78.46	0.38
Status*Site type	2.63	78.83	0.08
Status*Growth form	0.09	78.42	0.77
R^2 marginal	0.42		
R^2 conditional	0.74		

$\delta^{13}C$

Random effect

Groups	Name	Variance	SD
Species	Intercept	1.66	1.29
Residual		1.17	1.08

Number of observations: 296. Groups: Species = 87

Fixed effect parameters estimates

	Estimate	SE	df	t-value	p-value
Intercept	-30.89	0.59	69.37	-52.53	< 0.001
Status -native	0.15	0.65	71.73	0.23	0.82
Site type -mesic	0.65	1.04	62.75	0.62	0.53
Site type -xeric	1.08	0.77	74.89	1.41	0.16
Growth form - woody	2.38	0.86	62.34	2.76	0.007
Status -native: Site type -mesic	1.61	1.10	66.18	1.47	0.14
Status -native: Site type -xeric	1.10	0.89	77.52	1.24	0.22
Status -native: Growth form - woody	-1.10	0.94	70.39	-1.17	0.25

Anova table

	F-value	df	p-value
Intercept	16748.88	69.79	< 0.001
Status	1.29	72.57	0.26
Site type	7.61	74.54	< 0.001
Growth form	14.94	73.69	< 0.001
Status*Site type	1.35	73.87	0.27
Status*Growth form	1.36	73.59	0.25
R^2 marginal	0.38		
R^2 conditional	0.73		

Appendix C

Model calculation to test traits trade-offs

Second-order polynomial linear mixed models (LMMs) were calculated only for significant correlations between traits ($p < 0.05$), setting the species as the random intercept factor. When models had quadratic term statistically significant ($p < 0.05$), we reported the variance and its associated standard deviation (SD) of the random factor, as well as the coefficients and associated standard error (SE), degrees of freedom (df), t and *p* values, and their marginal and conditional R^2. In the case the quadratic term was not statistically significant, we computed a simple LMMs after testing for potential significant change in the residual sum of squares by means of likelihood ratio rest. The output of these analyses is reported below.

Ψ_{tlp} ~ LMA

Random effect

Groups	Name	Variance	SD
Species	Intercept	0.23	0.48
Residual		0.08	0.28

Number of observations: 351. Groups: Species = 95

Fixed effect

	Estimate	SE	df	t-value	p-value
Intercept	-1.78	0.05	90.00	-33.88	< 0.001
LMA (linear term)	-1.60	0.52	345.43	-3.08	0.002
LMA (quadratic term)	1.08	0.45	332.15	2.39	0.02
R^2 marginal	0.04				
R^2 conditional	0.75				

N_{mass} ~ LMA

Random effect

Groups	Name	Variance	SD
Species	Intercept	0.37	0.61
Residual		0.20	0.45

Number of observations: 351. Groups: Species = 95

Fixed effect

	Estimate	SE	df	t-value	p-value
Intercept	2.23	0.07	79.30	32.33	< 0.001
LMA (linear term)	-6.39	0.79	337.79	-8.09	< 0.001
LMA (quadratic term)	2.58	0.69	344.43	3.72	<0.001
R^2 marginal	0.19				
R^2 conditional	0.72				

VLM ~ LMA

Random effect

Groups	Name	Variance	SD
Species	Intercept	1826.1	42.73
Residual		986.2	31.40

Number of observations: 351. Groups: Species = 95

Fixed effect

	Estimate	SE	df	t-value	p-value
Intercept	138.13	4.87	87.66	28.34	< 0.001
LMA (linear term)	-825.75	55.57	339.17	-14.85	< 0.001
LMA (quadratic term)	421.15	48.71	344.48	8.64	<0.001
R^2 marginal	0.47				
R^2 conditional	0.81				

$\delta^{13}C$ ~ LMA

Random effect

Groups	Name	Variance	SD
Species	Intercept	1.43	1.20
Residual		0.87	0.93

Number of observations: 351. Groups: Species = 95

Fixed effect

	Estimate	SE	df	t-value	p-value
Intercept	-29.18	0.14	71.09	-203.88	< 0.001
LMA (linear term)	14.66	1.65	301.93	8.90	< 0.001
LMA (quadratic term)	-7.87	1.43	323.83	-5.53	<0.001
R^2 marginal	0.27				
R^2 conditional	0.72				

N_{mass} ~ Ψ_{tlp} (a)

Random effect

Groups	Name	Variance	SD
Species	Intercept	0.57	0.75
Residual		0.20	0.44

Number of observations: 351. Groups: Species = 95

Fixed effect

	Estimate	SE	df	t-value	p-value
Intercept	2.26	0.08	91.60	27.30	< 0.001
Ψ_{tlp} (linear term)	4.85	0.93	339.93	5.20	< 0.001
Ψ_{tlp} (quadratic term)	1.23	0.78	343.85	1.58	0.11
R^2 marginal	0.09				
R^2 conditional	0.77				

N_{mass} ~ Ψ_{tlp} (b)

Random effect

Groups	Name	Variance	SD
Species	Intercept	0.59	0.77
Residual		0.19	0.44

Number of observations: 351. Groups: Species = 95

Fixed effect

	Estimate	SE	df	t-value	p-value
Intercept	3.01	0.16	294.34	17.69	< 0.001
Ψ_{tlp}	0.41	0.08	346.34	4.92	< 0.001
R^2 marginal	0.09				
R^2 conditional	0.77				

LR Test (N_{mass} ~ Ψ_{tlp} (a) vs N_{mass} ~ Ψ_{tlp} (b): p = 0.11

VLM ~ Ψ_{tlp} (a)

Random effect

Groups	Name	Variance	SD
Species	Intercept	4745	68.89
Residual		1408	37.53

Number of observations: 351. Groups: Species = 95

Fixed effect

	Estimate	SE	df	t-value	p-value
Intercept	143.86	7.52	294.34	17.69	< 0.001
Ψ_{tlp} (linear term)	202.82	80.91	344.30	2.51	0.01
Ψ_{tlp} (quadratic term)	90.22	67.32	340.42	1.34	0.18
R^2 marginal	0.02				
R^2 conditional	0.78				

VLM ~ Ψ_{tlp} (b)

Random effect

Groups	Name	Variance	SD
Species	Intercept	4764	69.02
Residual		1411	37.56

Number of observations: 351. Groups: Species = 95

Fixed effect

	Estimate	SE	df	t-value	p-value
Intercept	173.35	14.85	296.04	11.67	< 0.001
Ψ_{tlp}	16.13	7.24	347.00	2.23	0.02
R^2 marginal	0.09				
R^2 conditional	0.77				

LR Test (VLM ~ Ψ_{tlp} (a) vs VLM ~ Ψ_{tlp} (b): $p = 0.19$

$\delta^{13}C$ ~ Ψ_{tlp}

Random effect

Groups	Name	Variance	SD
Species	Intercept	2.48	1.58
Residual		0.93	0.97

Number of observations: 351. Groups: Species = 95

Fixed effect

	Estimate	SE	df	t-value	p-value
Intercept	-29.28	0.18	75.58	-161.42	< 0.001
Ψ_{tlp} (linear term)	-6.24	2.05	310.10	-3.04	< 0.001
Ψ_{tlp} (quadratic term)	-4.54	1.72	323.67	-2.64	0.008
R^2 marginal	0.08				
R^2 conditional	0.74				

N_{mass} ~ VLM (a)

Random effect

Groups	Name	Variance	SD
Species	Intercept	0.42	0.65
Residual		0.18	0.42

Number of observations: 351. Groups: Species = 95

Fixed effect

	Estimate	SE	df	t-value	p-value
Intercept	2.25	0.07	86.57	30.91	< 0.001
VLM (linear term)	7.55	0.86	326.67	8.76	< 0.001
VLM (quadratic term)	0.38	0.57	303.52	0.66	0.51
R^2 marginal	0.21				
R^2 conditional	0.77				

N_{mass} ~ VLM (b)

Random effect

Groups	Name	Variance	SD
Species	Intercept	0.42	0.64
Residual		0.18	0.42

Number of observations: 351. Groups: Species = 95

Fixed effect

	Estimate	SE	Df	t-value	p-value
Intercept	1.53	0.11	199.31	13.93	< 0.001
Ψ_{tlp}	0.05	0.01	335.94	9.10	< 0.001
R^2 marginal	0.22				
R^2 conditional	0.76				

LR Test (N_{mass} ~ VLM (a) vs N_{mass} ~ VLM (b): p = 0.52

$\delta^{13}C$ ~ VLM (a)

Random effect

Groups	Name	Variance	SD
Species	Intercept	2.01	1.42
Residual		0.90	0.95

Number of observations: 351. Groups: Species = 95

Fixed effect

	Estimate	SE	df	t-value	p-value
Intercept	-29.25	0.16	77.20	-176.89	< 0.001
VLM (linear term)	-12.35	1.88	306.79	-6.56	< 0.001
VLM (quadratic term)	1.87	1.27	283.42	1.48	0.14
R^2 marginal	0.14				
R^2 conditional	0.73				

$\delta^{13}C$ ~ VLM (a)

Random effect

Groups	Name	Variance	SD
Species	Intercept	2.07	1.44
Residual		0.90	0.95

Number of observations: 351. Groups: Species = 95

Fixed effect

	Estimate	SE	df	t-value	p-value
Intercept	-28.08	0.25	183.15	-110.53	< 0.001
VLM	-0.008	0.01	316.96	-6.35	< 0.001
R^2 marginal	0.14				
R^2 conditional	0.73				

LR Test ($\delta^{13}C$ ~ VLM (a) vs $\delta^{13}C$ ~ VLM (b): $p = 0.52$